*Appraisal of Temporal Variations in Atmospheric Compositions over South Asia by Addition of Various Pollutants in Recent Decade

*A Study of Active Chaman Fault System (CFS) using SRTM DEM

*SRTM DEM based Neotectonics from Non-Linear Analysis: A Paradigm through Fractal Analysis

Journal.50sea.com

Prof Dr. Ali Iqtadar Mirza
Chief Editor
International Journal of Innovations in Science and Technology

Abstracting and Indexing

IJIST
P ISSN : 2618-1630
E ISSN : 2909-6130
Recognized Journal

Scientific Journal Impact Factor
TOGETHER WE REACH THE GOAL

Scilit

CiteFactor
Academic Scientific Journals

IOI JOURNALS MASTER LIST

IDEAS

INFOBASE INDEX

IPIndexing
Indexing Portal

RESEARCHBIB
ACADEMIC RESOURCE INDEX

ROOTINDEXING
JOURNAL ABSTRACTING AND INDEXING SERVICE

SIS

WIKIDATA

Instructions for Authors

The editorial board encourages and welcome true researches, laboratory experiments and real time field observations to get published in IJIST. The authors are advised to prepare their manuscript according to the template of IJIST.

Please see the checklist before submitting your manuscript to IJIST.

- The manuscript is prepared according to the template of IJIST.
- Symbols and names are used according to international standards.
- Page no and Line no are adjusted on the manuscript.
- Figure and Table are clearly cited.
- Author names and their affiliation are typed clearly.
- There is no any limit to the length of manuscript.
- Abstract is comprised of 250 words.
- Author's contribution and the statement narrating no of conflict of interest is mentioned in the end.
- Each Figure and Table is numbered and cited in the text.
- Spelling and English grammar is checked.
- It is "Open Access" journal that publish articles on payment of publishing fee by authors or by their institutions.
- All the articles are published under Creative Common License CC-BY therefore, authors mush agree with same license.

Aims and Scopes

The authors are advised to submit their manuscript in accordance with disciplines as below:

- Administrative Science
- Agriculture/Forestry
- Climatology
- Criminology
- Development Study
- Environment
- GIS
- Geography
- Meteorology
- Physics
- Remote Sensing
- Social Science
- Urban Planning
- Economics
- Chemistry
- Bio-Chemistry
- Computer Science

Peer Review Process

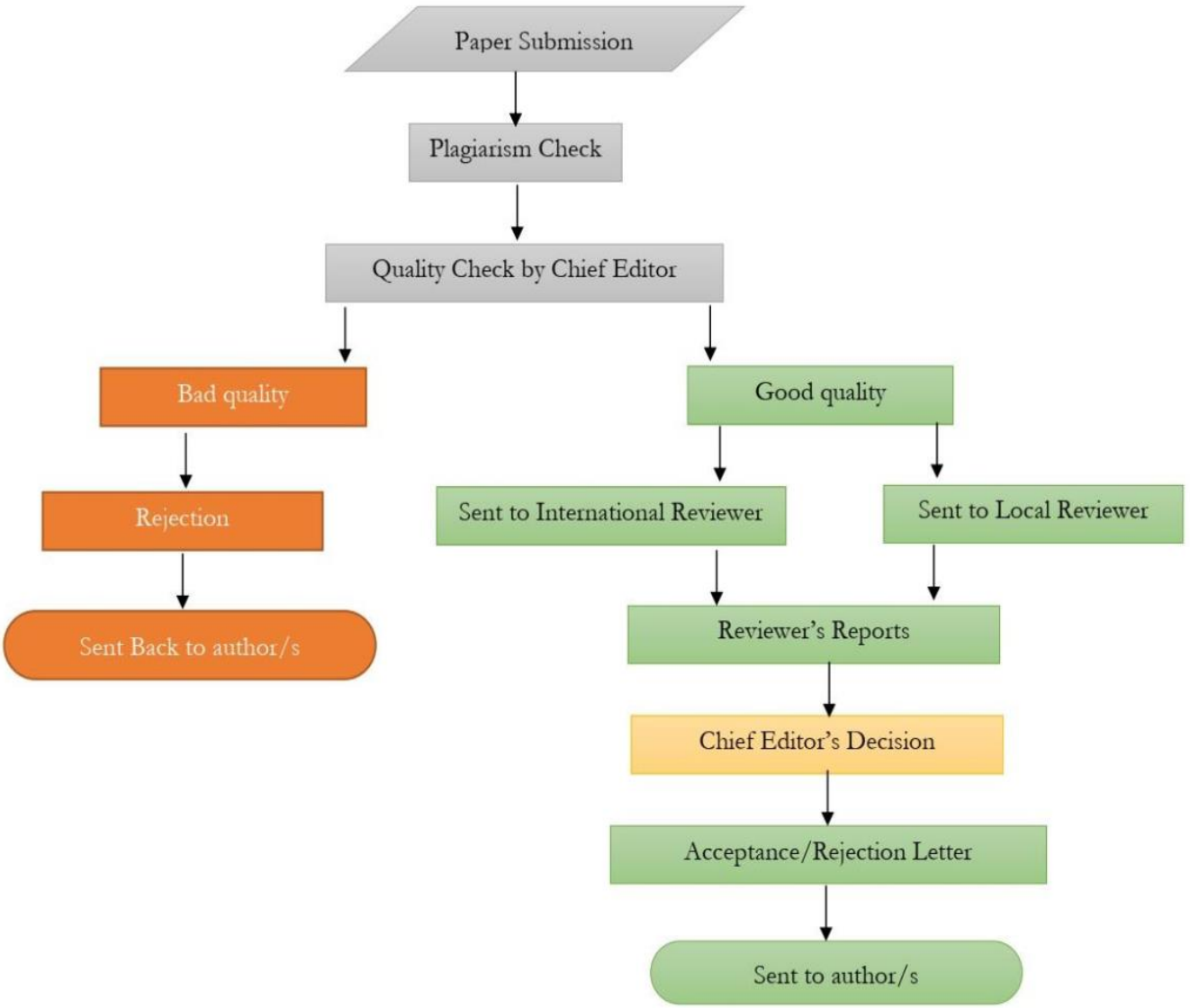

Table of Contents

International Journal of Innovations in Science & Technology (IJIST)

ISSN 2618-1630

V3-I1 | March 2021

IJIST
P ISSN : 2618-1630
E ISSN : 2909-6130

Appraisal of Temporal Variations in Atmospheric Compositions over South Asia by Addition of Various Pollutants in Recent Decade

Ehsan UL Haq[1], Farwah Waseem[1], Abdul Baqi[2]
[1] Department of Space Science (University of The Punjab).
[2]Goverment Degree College Usta Muhammad, District Jaffarabad, Balochistan, Pakistan
* Correspondence: Ehsan UL Haq[1] (rana42ehsan@gmail.com).

Citation | Haq.U.E, Waseem.F, Baqi.A," Appraisal of Temporal Variations in Atmospheric Compositions over South Asia by Addition of Various Pollutant's in Recent Decade". International Journal of Agriculture & Sustainable Development, Vol 03 Issue 01: pp 01-15, 2021.
Received | Jan 12, 2021; Revised | Jan 29, 2021 Accepted | Feb 04, 2021; Published | Feb 08, 2021.

Abstract.

Atmosphere is an envelope of gasses and aerosols around the planet, 99% of the total mass of atmospheric gases resides within 32km from Earth's surface in vertical column. From primordial era to current scenario composition of earth endured numerous drastic modifications. In last decade atmosphere had undergone a vigorous change by the addition of many pollutants in both natural and anthropogenic aspects. South Asia is a densely populated; masses here are in a transition state, these developing nations in this region considerably done enough damage to the atmosphere of south Asia by inserting multiple pollutants in atmosphere in a number of anthropogenic activities. These pollutants piled up as a serious danger for people around the globe like Methane (CH4), Sulphur Dioxide (SO_2), Carbon Monoxide (CO) Nitrogen Dioxide (NO2), Carbon Dioxide (CO2), Formaldehydes (HCHO) and tropospheric Ozone (O3) etc. "Environmental Remote Sensing" has arisen as a great tool of modern era to get fruitful and precise results to monitor these variations in atmospheric pollutants. The NASA's (National Aeronautics and Space Administration), Geospatial Interactive Online Visualization ANd aNalysis Infrastructure (Giovanni) system provides access to a wide variety of NASA's remote sensing data, Variety of environmental data types has permitted the use of Giovanni for different applications to define addition and increase in concentration of various pollutants. Spatio temporal variation of pollutants shows their concentration increased in last decade and in last three years the concentration boosted as compared to last seven years.

Keywords: Anthropogenic, Pollutants, Environmental Remote Sensing. National Aeronautics and Space Administration (NASA), Geospatial Interactive Online Visualization ANd aNalysis Infrastructure (Giovanni).

INTRODUCTION

The earlier atmosphere of earth was composed of gasses like Ammonia, Methane, water vapors and Neon while Oxygen was pretty lack in concentration in primordial state, which proved to be the most important biological component for the composition of current atmosphere [1]. The atmosphere consisting of primordial gases is highly dependent upon the gravitational pull of the planet, this gravitational force holds the atmospheric components together, thus some of energy and speed is required to escape this gravitational pull, this speed is expressed as escape velocity [2].

If we consider a formula to explain the primordial gases, velocity of the gas molecules is directly relational to (T/M)/2

T= Total temperature of the molecule in Kelvin (K)

M= Molar mass of the molecules

The temperature below 2000K and molar mass of a molecules greater than 10 would have velocity less than 11.3 km, shows molecule might be stayed in the primordial atmosphere, from this observation we can conclude; Hydrogen and Helium have molar mass less than 10 (2 and 4 respectively) therefore, these couple of gasses are lost in universe [3]. Methane, Ammonia, water vapors and Neon have molar mass greater than 10 therefore, these might be a part of primordial gases in the early atmosphere. The present-day main constituents of atmosphere are: molecular nitrogen (N_2) & molecular oxygen(O_2) and Noble gasses including Helium (He), Neon (Ne), Argon (Ar), Krypton (Kr), and Xenon (Xe). The variable constituents abundant in the concerned scenario are liquid vapor (H_2O) and carbon dioxide (CO_2) [4], rest of the components are in lesser amounts in current scenario: Nitrogen-Dioxide (NO_2), Hydrogen-Sulfide (H_2S), Sulfur-Dioxide (So_2), Hydrogen-Chloride (Hcl), Molecular-Hydrogen(H_2), Methane (Ch_4), Carbon-Monoxide (CO), Ammonia (NH_3), Nitrous-Oxide (N_2o). Nitrogen (N_2) occupies 78% of atmospheric composition in form of compounds like encompassing ammonium ($NH+$), nitrite (NO_2-) and nitrate (NO_3-). The conversion of nitrogen into these compounds is known as nitrification [4,5]. Ammonia is transformed by the bacterial reaction that was latterly used by the plants for growth, eventually that ammonia used by the plants produce N_2. The petroleum products that are used in daily life to drive many things, produce oxides of nitrogen which finally leads to N_2. Fog in urban areas is also nitrous oxides [5]. Natural processes including volcanic eruption and weathering of the rocks containing sulfur adds sulfur dioxide (SO_2) and sulfate (SO_4) into the atmosphere. Sulfur dioxide reacts with water to become highly corrosive sulfuric acid (H_2SO_4). In the beginning of industrial era, anthropogenic events by human added enough sulfur into atmosphere by burning of fossil fuels [6]. Industrial setups deposited sulfur and nitrogen into atmosphere which precipitated into sulfuric acid, nitrogen oxides and to nitric acid (HNO_3), leading to acidic rain. The CO_2 is attained trough many processes including the respiration of the living things, by the weathering of the rocks containing carbon and volcanic eruptions. The fossil fuel burning and advanced industrial development has increased the CO_2 deposition in atmosphere, which resultantly increased the temperature of the troposphere, in a process commonly known as global warming. Many anthropogenic activities and multiple natural resources boosted the concentration of pollutants in atmosphere including tail pipe emission,

volcanic eruption, fossil fuel burning etc. Anthropogenic activities have changed the chemical composition of our atmosphere that has influenced the Earth's atmospheric composition [7].

Aerosols is defined as a fine suspension of the particles or liquid droplets in atmosphere, it might be natural or anthropogenic i.e., dust, wood land burning, fog, volcanic eruptions etc [8]. Primary aerosols have the particles that are directly developed into the gas, while the secondary one contains the particles which are evolved from the gas, there are many sorts of aerosols which are classified depending upon the particle size. The Aerosole Index (AI) can be discriminated accurately among absorbing and non-absorbing aerosols depending upon the extent of absorption of UV radiation [9]. The positive values that is related with AI is mostly the absorbing aerosols and vice versa. Anthropogenic aerosols are air pollutants, haze and smoke, these particles have the diameter normally greater than 1μm, and their significant settling velocity is enough to keep this stuff as a mixture.

Ozone is a trioxygen organic molecule, having pale blue color with a pungent smell, an allotrope of oxygen. It exists in low concentration in troposphere and have high concentration in ozone layer in stratosphere and engages maximum UV from sun [10].

$$NO + O_3 \rightarrow NO_2 + O_2$$
$$NO_2 + O_3 \rightarrow NO_3 + O_2$$
$$C + 2O_3 \rightarrow C\,O_2 + 2O_2$$
$$3\,SO_2 + 3\,H_2O + O_3 \rightarrow 3\,H_2SO_4$$
$$H_2S + O_3 \rightarrow SO_2 + H_2O$$
$$O + O_2 + M \rightarrow O_3 + M$$
$$O_3 \rightarrow O + O_2 + \text{kinetic energy}$$

Sulphur dioxide is a toxic gas with smell like burnt matches. It originates from volcanos, scorching of fossil fuels & biomass, having formula SO_2. It exists in Earth's atmosphere in a very small concentration about 1 ppm [11].

$$2\,SO_2 + 2\,H_2O + O_2 \rightarrow 2\,H_2SO_4$$

Several oxides of nitrogen exists, but here we are concerned with the nitrogen dioxide with formula NO_2. It is the main agent used in production of nitric acid in industry, at high temperature. It is a reddish-brown gas with prominent irritating odor.

$$2\,NO + O_2 \rightarrow 2\,NO_2$$

It is produced when nitric oxide reacts with the molecular oxygen.

$$2NO_2 \rightarrow 2NO + O_2$$

NO_2, is added into troposphere by some natural sources, bacterial respiration, lightning, volcanos and from stratosphere. It is prominent absorber of sunlight. Anthropogenic activities like, combustion in engine, fossil fuel, cigarette smoke, stoves and kerosene heaters also add NO_2 in atmosphere [10, 11].

CO is a colorless, odorless, and tasteless gas, highly flammable having density less than air. It is a toxic gas, therefore it is known as a pollutant of atmosphere. It is produced during metabolism of animals and released in the atmosphere; it is a short lived spatially variable, which causes to produce tropospheric ozone [12].

$$CO + 2O_2 + h\nu \rightarrow CO_2 + O_3$$

Its sources are carbon oxidation, stove, and engine combustion, iron smelting, photochemical reactions in the atmosphere, volcano, wild fire and breakdown of hemoglobin.

Methane is the main part of the natural gas and considered as important fuel. It exists in form of gas in normal conditions. Mostly exists under the seafloor and produced in couple of processes i.e. geological and biological processes [13].

It is used in combustion

$$CH_4 + 2\ O_2 \rightarrow CO_2 + 2\ H_2O$$

$\Delta H = -891$ kJ/moll, at standard conditions

Reaction with water

$$CH_4 + H_2O \rightleftharpoons CO + 3H_2$$

The concentration of atmospheric methane has been amplified by 150% since 1750. It owns a prime importance due to its greenhouse effect with huge global warming potential as compared with other agents of atmospheric heat trapping gases including CO_2.

Formaldehyde is an organic compound with the formula H−CHO. It seems dated in the upper atmosphere, it is intermediate in oxidation of methane, which is produced in presence of sunlight by chemical reaction of methane with oxygen. Due to its wide use, volatility and toxicity, formaldehyde is dangerous for human health [8,11,13].

Carbon dioxide exists in the atmosphere of earth as a trace gas, it is colorless gas which is 60% dense than dry air, originate from volcano, carbonate rocks, ground water, rivers, lakes, ice caps, natural gas, tail pipe emissions and petroleum. It is odorless gas. It is also produced by the process of respiration, decay of organic matter and combustion of fossil fuel. It is also a greenhouse gas, by the industrial revolution, deforestation and combustion of organic materials enhanced the concentration of carbon dioxide which lead to the global warming [14].

The above discussion verifies that tropospheric concentration of multiple pollutants is formed by photochemistry of toxic pollutants in the atmosphere. Summer season is proved favorable to enhance the concentration of these pollutants. The elevated temperature act as catalyst in all chemical reactions like oxidation or reduction of hydrocarbons, and the oxides of nitrogen, carbon and Sulphur which are commonly known as Ozone precursors. These oxides play a vital role in the formation of pollutants through complex chemical reactions. Therefore, it is significant to investigate the participation of precursors in formation of pollutants. The optimum range of these precursors is important to maintain a healthy environment [15, 16, 17].

The specific objective of this research was to map the spatiotemporal variations in concentration of atmospheric pollutants from 2009 to 2019 over South Asia. It also aims at describing the contribution of precursors in pollutant formation by direct or indirect chemical reactions. This research will open new avenues for scientists and researchers to control various toxic pollutants for a sustainable regional environment.

Material and Methods.

Investigation site. South Asia cover-ups an area approximately 5.2 million km^2 area that is 11.71% of the Asian continent by percentage or 3.5% of the world's area carrying huge number of messes on it, it is residential land of approximately 1.9 billion people.

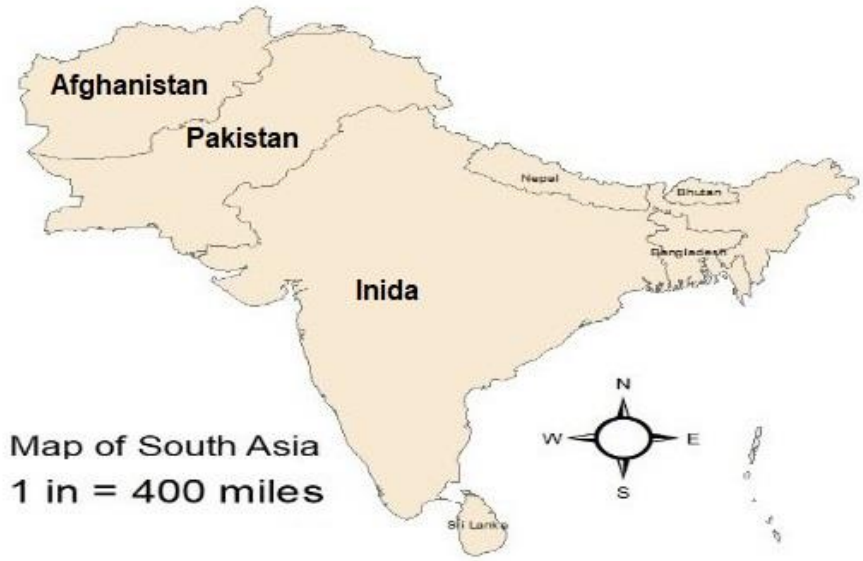

Figure 1. Map of south Asia.

This region consists of eight countries according to the South Asian Association for Regional Cooperation (SAARC) including Pakistan, India, Afghanistan, Bhutan, Nepal, Sri Lanka, Maldives and Bangladesh [18].

South Asia becomes extremely hot in April and May according to the native masses. Temperature rises upto 100°F, air becomes full of dust, ponds dry up. Just in couple of hours, rivers run-off their banks, latterly land dries out, this scenario seems dated every year in south Asia [18].

South Asia contains six foremost climate zones, the mountainous regions where snow remains present whole year, having coldest climate. It is a region of high temperature and mild rainfall and considered as semiarid zone, found in western end of the plain, extends to the desert along Pakistan and India.

Material and methods.

The Data was acquired from GIOVANNI (AIRS On boarded on AQUA & OMI On boarded on AQUA) data archives. Parameters regarding atmospheric compositions were defined from the above-mentioned data archives, to explain the variations in a decade over this huge area of South Asia. Remote sensing data from different satellites is vital for evaluating the natural events in our atmosphere at a regional scale or worldwide. This info is exploited to determine changes in enduring decade [20]. The assortment of environmental data types which allows an individual to use Giovanni for different purposes, like atmospheric composition etc. [21].

Aura is a successor to the atmospheric instruments. It was launched in a near polar orbit at an inclination of 98 degrees in a sun synchronous trajectory, orbits with a retro of 100 minutes. Aura repeat its ground track in 16 days, orbiting at a height of 705 km with local time to cross equator at 1.45 pm [39]. OMI (Ozone monitoring instrument), housed on Aura. This sensor is much accurate to differentiate among the aerosol categories, like smoke & dust etc.

and provides data about tropospheric ozone, cloud coverage and its pressure. This instrument uses hyperspectral imaging in push-broom mode to observe the back scatter radiations illuminated by the sun in the visible and ultraviolet. It is efficient to monitor the atmospheric ozone, aerosols, atmospheric dust, NO_2 & smoke [22].

Aqua was launched on May 4, 2002, having near polar sun-synchronous circular orbit, with inclination of 98.2º. It orbits at 705 km, local time to cross equator is 1:30 PM, its period is 98.8 minutes and repeat its cycle in 16 days with a swath width of 1650 km (± 49.5 degrees) [23].

AIRS (Atmospheric Infra-Red Sounder) with AMSU (Advanced Microwave Sounding Unit) mounted on Aqua, is helpful in observing the tropospheric column of the atmosphere, from ground level to the top of atmosphere [24]. Data from Giovanni is assembled with respect to its applicability regarding atmospheric composition.

Tier data parameters are as follows,

UV Aerosol Index	Carbon Dioxide mole fraction in troposphere
Methane Mole fraction in Air	Sulphur dioxide tropospheric column
Carbon monoxide Mole fraction in troposphere	Ozone Mole fraction in Air
Formaldehydes Tropospheric column	Nitrogen dioxide tropospheric column
Air temperature	

Result and discussion

The results show that spatio-temporal variations in atmospheric composition occurred by an increase in concentration of multiple pollutants in last decade. The area was monitored in four-time frames of a year, pre-monsoon, monsoon, post-monsoon and winter or dry season.

Aerosol Index

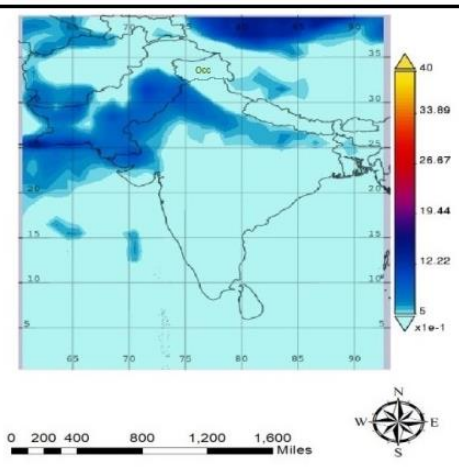

Figure 2. Map of UV Aerosol Index (AI) average of daily observation with spatial resolution 1 deg (Jan-1-2009 to Dec-31-2019) by OMI

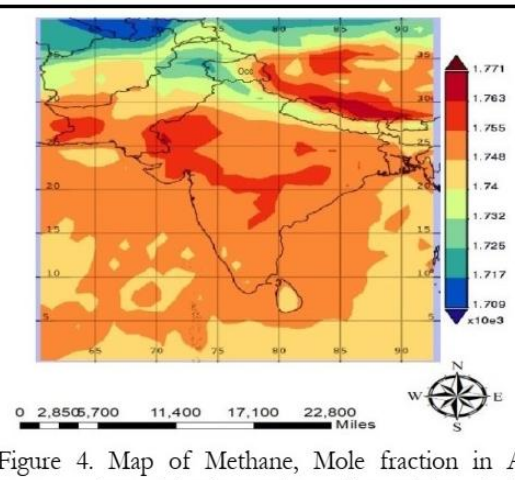

Figure 4. Map of Methane, Mole fraction in Air, average of monthly observation with spatial resolution 1 deg (Jan-1-2009 to Dec-31-2019) by AIRS

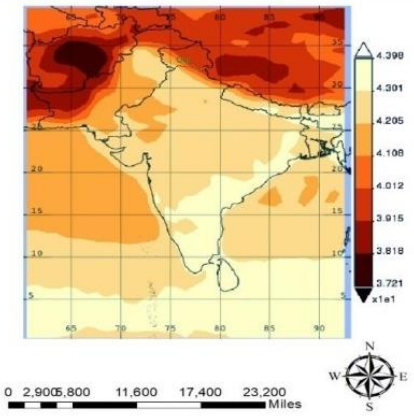

Figure 6 Map of Carbon Monoxide, Mole fraction in Air, average of monthly observation with spatial resolution 1 deg (Jan-1-2009 to Dec-31-2019) by AIRS

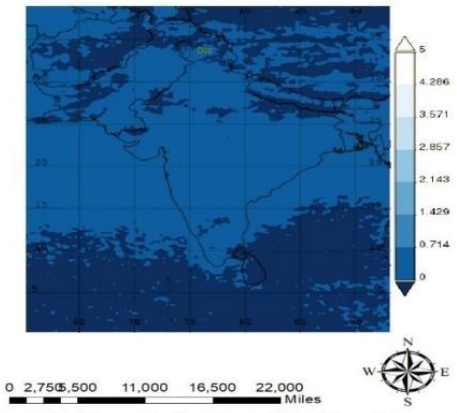

Figure 8 Map of Sulphur Dioxide, Tropospheric Colum, average of daily observation with spatial resolution 0.25 deg (Jan-1-2009 to Dec-31-2019) by OMI

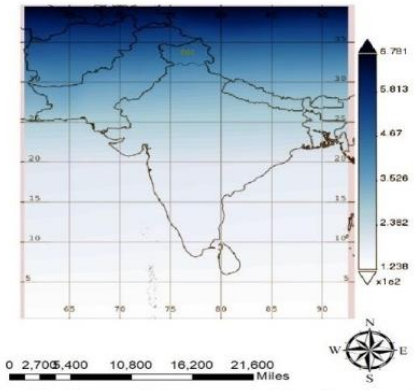

Figure 10 Map of Ozone, Mole fraction in Air, average of monthly observation with spatial resolution 1 deg (Jan-1-2009 to Dec-31-2019) by AIRS

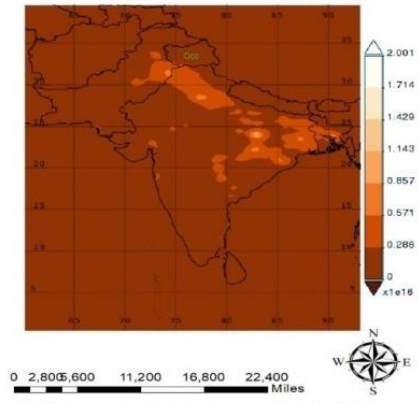

Figure 12 Map of NO_2, Tropospheric Colum, average of daily observation with spatial resolution 0.25 deg (Jan-1-2009 to Dec-31-2019) by OMI

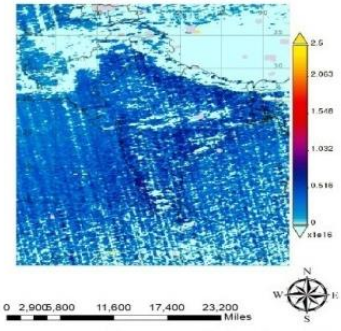

Figure 14 Map of Formaldehydes, Tropospheric Colum, average of daily observation with spatial resolution 0.1 deg (Jan-1-2009 to Dec-31-2019) by OMI

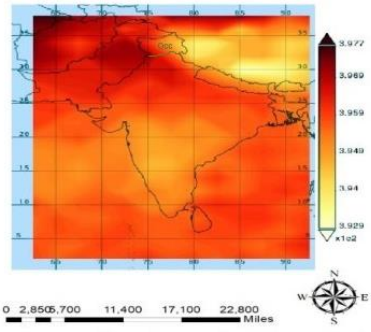

Figure 16 Map of Carbon Dioxide mole fraction in troposphere (IR only), average of monthly observation with spatial resolution 2*2.5 deg (Jan-1-2009 to Dec-31-2017) by AIRS

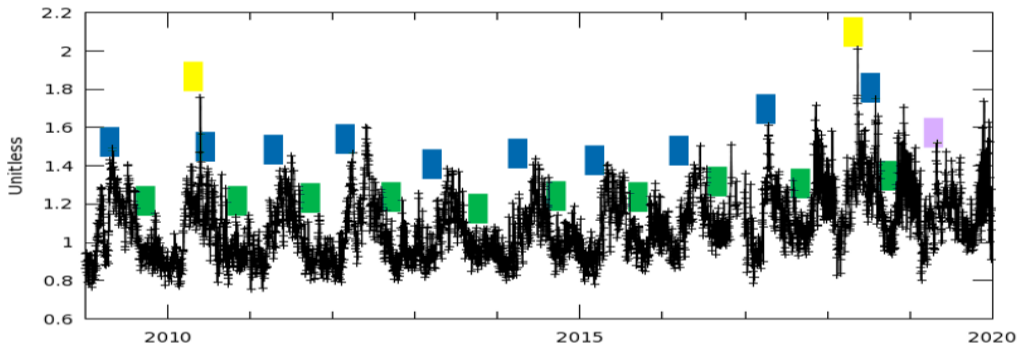

Figure 3. Temporal variation of UV Aerosol Index (AI) average of daily observation with spatial resolution 1 deg (Jan-1-2009 to Dec-31-2019) by OMI

Figure 2, is showing that the concentration of aerosols increased in bulk on eastern, north-eastern side, costal line at south and North-Western side of Pakistan, and western side of India along Himalayan basin. It is due to wind system in subcontinent and 4 seasons that seems dated every year. In South Asia, the month of April and May is quite hot and dry, winds in these couple of months changes their direction from sea towards land, known as easterlies, wind gusts i.e., huge mass of air invades into plan area of subcontinent with continuous increase in temperature. This area looks like a burning Incinerator during these months, it's also harvesting time of Rabi crops, dust from these crops harvesting and smoke after burning their residue, make environment full of multiple aerosols. Winds changes their direction from land towards sea (Westerlies) in October and November which is considered a stable condition but with full smokey stuff, post harvesting of kharif crop in these months (post monsoon) the residue burn, their smoke and different hazardous gasses originate during burning and suspend in to the atmosphere and make the complete environment full of aerosols.

Methane

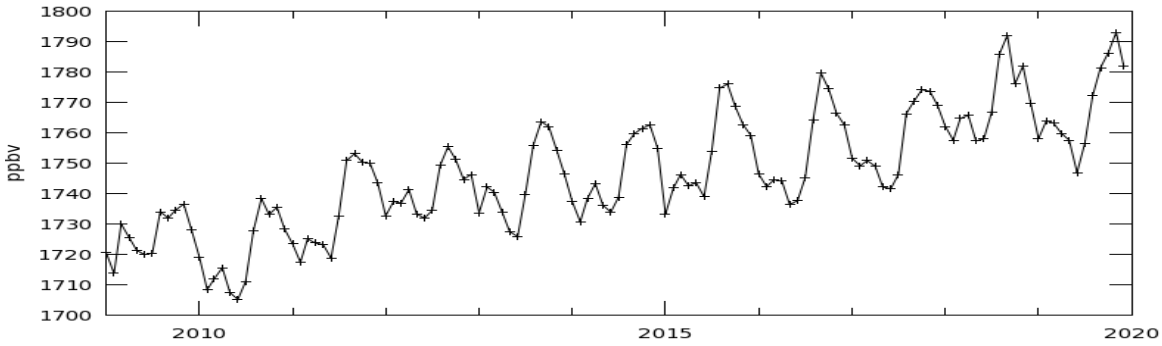

Figure 5. Temporal variations of Methane, Mole fraction in Air, average of monthly observation with spatial resolution 1 deg (Jan-1-2009 to Dec-31-2019) by AIRS

Figure 3 shows the temporal distribution of aerosols during last decade, the peaks along blue represents UV-Al maximum in this season later on in monsoon precipitation at its peak and this area faces heavy down pour in the month of June, July and August that wash out the pollutants from atmosphere. The dips in green bars represent the concentration of aerosols after monsoon which is pretty low as compared to pre-monsoon. In post-monsoon

(Oct and Nov) winds get calm and precipitation is low, peaks in figure show heavy loading in post-monsoon which leads to Smog, later on in winter again precipitations started, due to rain, dew and frost, these pollutants settled down and by the end of each year, their graph is at its lowest value.

Hotspots in Figure 4 are showing the spatial distribution of methane over south Asia, orange shaded area in India and south western border among India and Pakistan shows methane amalgamation in air, as we know, it's a natural gas, that exist in marshy areas and under sea floor which react with water. Figure 5 is showing the annual variations in methane concentration in recent decade, methane concentration was noted low in winter season. The peaks in each year in pre-monsoon show a small loading of methane, later on in mon-soon, methane particles were washed out due to heavy rain, in post-monsoon we can see that figure got maximum height in each year, that shows huge concentration of methane in post monsoon. But overall representation of graph is showing an increasing trend in concentration of methane as its increased by 150% since 1970.

Carbon monoxide

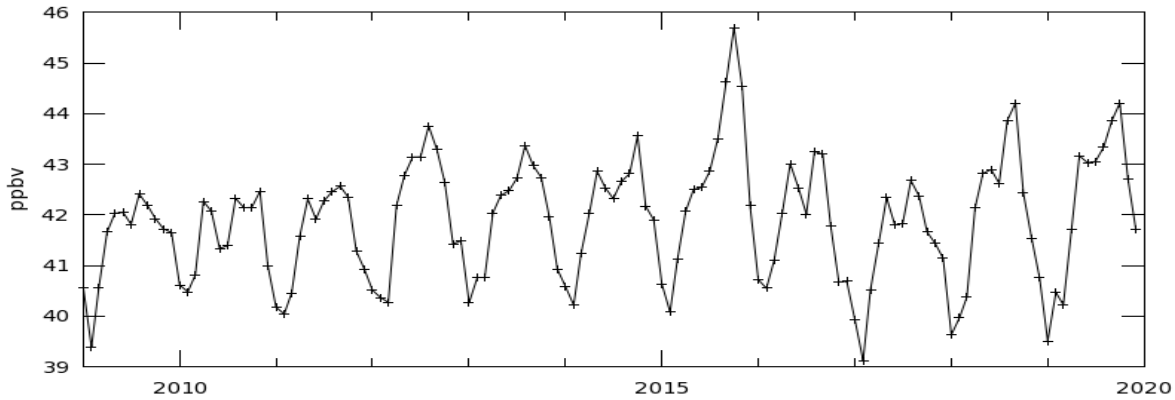

Figure 7. Temporal variations of Carbon Monoxide, Mole fraction in Air, average of monthly observation with spatial resolution 1 deg (Jan-1-2009 to Dec-31-2019) by AIRS.

Map of carbon monoxide in Figure 6 is showing its spatial distribution. Figure 7 is showing the variations of CO in air in recent decade, the change in concentration was observed from 42 to 44 ppbv in air. In context of seasonal variations, it remains same whole year except in winter (low in concentration) as shown in figure 6. It is a main source for the production of tropospheric Ozone which is a highly toxic gas. Figure 7 is showing an increasing trend of CO from 2009 to 2019 which may be due to certain reactions of atmospheric fresh oxygen with carbon residuals in the atmosphere. The concentration of Carbon aerosols is increasing in the atmosphere due to anthropogenic activities which may interact with oxygen.

Sulphur Dioxide

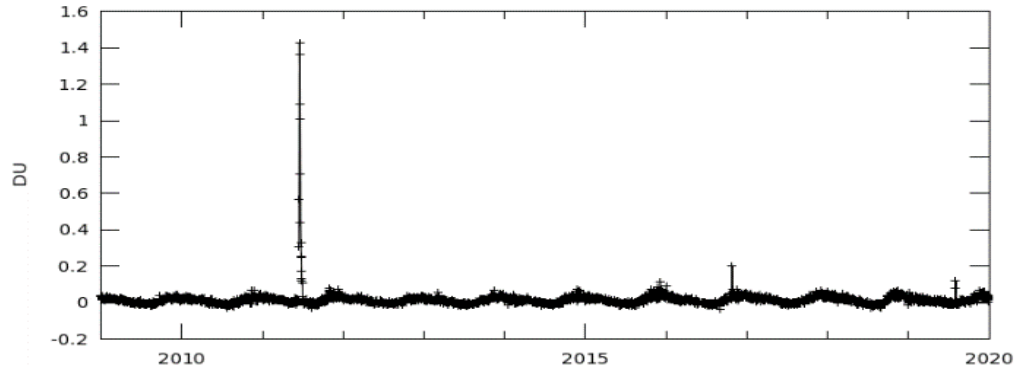

Figure 9. Temporal variations of Sulphur Dioxide, Tropospheric Colum, average of daily observation with spatial resolution 0.25 deg (Jan-1-2009 to Dec-31-2019) by OMI

Figure 8 shows that the concentration of Sulphur Dioxide has been increased in recent decade, being a short-lived pollutant it reacts with water vapor's which leads to formation of Sulphuric acid (acidic rain). Figure 9 shows temporal distribution in concentration of Sulfur dioxide which is observed changed from 0.05 to 0.2 DU. Only 30% of this pollutant is produced in natural processes rest of the 70% is the reward of anthropogenic activities.

Ozone

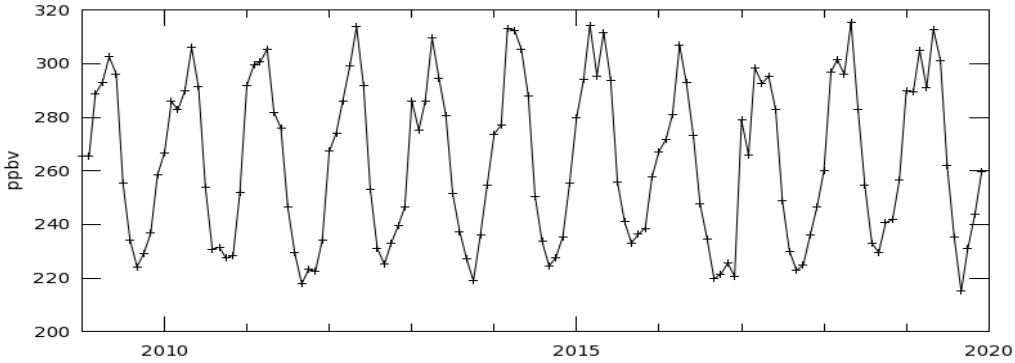

Figure 11. Graphical Representation of Ozone, Mole fraction in Air, average of monthly observation with spatial resolution 1 deg (Jan-1-2009 to Dec-31-2019) by AIRS

Ozone is an oxidizing agent, tropospheric ozone is pretty harmful for health, but its concentration is increased from 280 to 318 ppbv in recent decade as shown in Figure 11. This figure shows that seasonal variation of ozone shows its decreasing concentration with the start of monsoon which raised again from post monsoon in winter. Figure 10 shows spatial distribution of ozone and its maximum concentration over populated area in sub-tropical region where anthropogenic activities were observed at peak (i.e. mega cities of subcontinent).

Nitrogen Dioxide

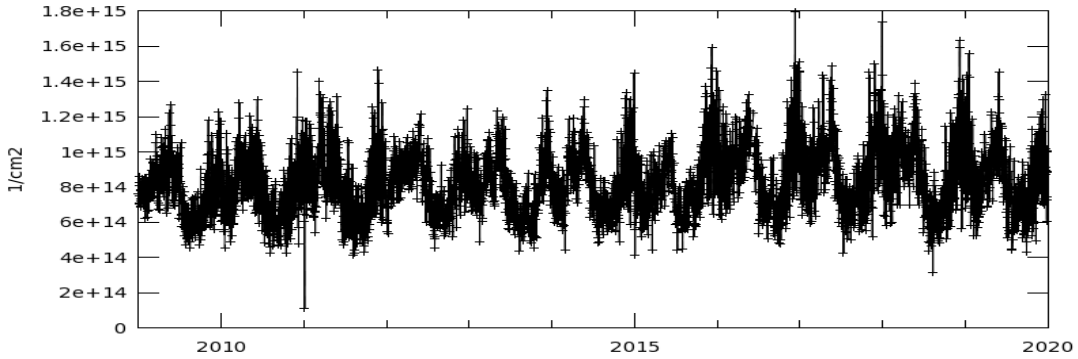

Figure 13. Temporal variations of Nitrogen Dioxide, Tropospheric Colum, average of daily observation with spatial resolution 0.25 deg (Jan-1-2009 to Dec-31-2019) by OMI

Nitrogen dioxide is a prime aerosol, and an absorber of sunlight, NO_2 in troposphere is a prominent pollutant. Its reaction with other atmospheric components (water vapors) results in formation of nitric acid and the sun light act as a catalyst. Figure 12 shows its spatial distribution over mega cities or densely populated area of south Asia (where maximum anthropogenic actives are undertaken). Figure 13 shows the temporal variation in Nitrogen Dioxide in recent decade, which raised in troposphere in pre and post monsoon. In monsoon, pollutants washed out so its concentration in troposphere seems low in winter and the tendency of this pollutants raised gradually up to pre monsoon.

Formaldehydes (HCHO)

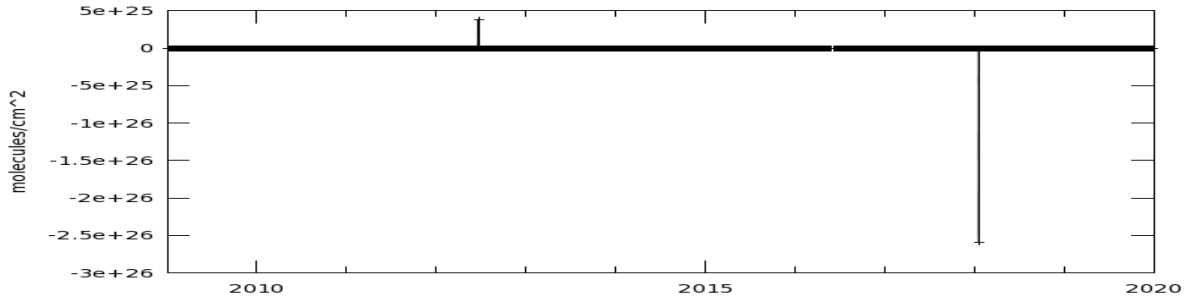

Figure 15. Temporal variations of Formaldehydes, Tropospheric Colum, average of daily observation with spatial resolution 0.1 deg (Jan-1-2009 to Dec-31-2019) by OMI

HCHO is toxic gas produced in the oxidation of methane, it is small in concentration in troposphere. The concentration of this pollutant is totally dependent upon temperature. Figure 14 and 15 shows its spatial and temporal variations in the previous decade, as it exists in small concentration therefore no considerable variations are observed.

Carbon Dioxide

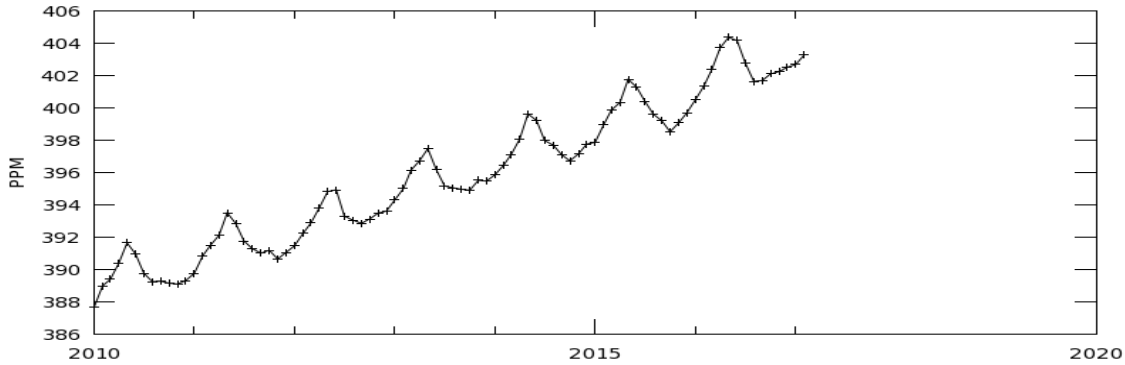

Figure 17. Temporal variations of Carbon Dioxide mole fraction in troposphere (IR only), average of monthly observation with spatial resolution 2*2.5 deg (Jan-1-2009 to Dec-31-2017) by AIRS

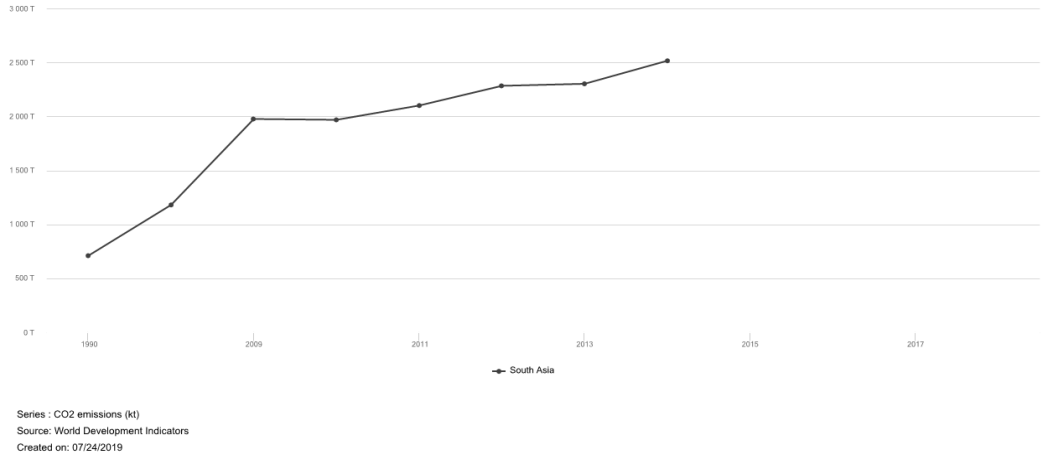

Figure 18. Carbon dioxide emission (KT) in south Asia (1990-2017). Source: World Bank Report

Carbon dioxide is a greenhouse gas, originate from several natural resources and anthropogenic activities, its concentration in troposphere was raised in last decade which caused global warming, Figure 17 is showing how its concentration was raised from 2010 to 2017 between a range 390 to 404 PPM in troposphere. The seasonal variations of this pollutant observed at peak in pre-monsoon and monsoon. Figure 16 shows spatial distribution of CO_2, in Pakistan and on border of Indian and Pakistani Punjab, this area is rich in agriculture and industry in Pakistan, so maximum production of CO_2 added from this area in to atmosphere. The anthropogenic activities include industrial waste, tail pipe emission, burning of crop residue and high temperature that work as a catalyst. According to WORLD BANK report, the annual emission of CO_2, has been enhanced from 1994 to 2014 from 600T to 2500T (T=TON) as shown Figure 18.

Air temperature

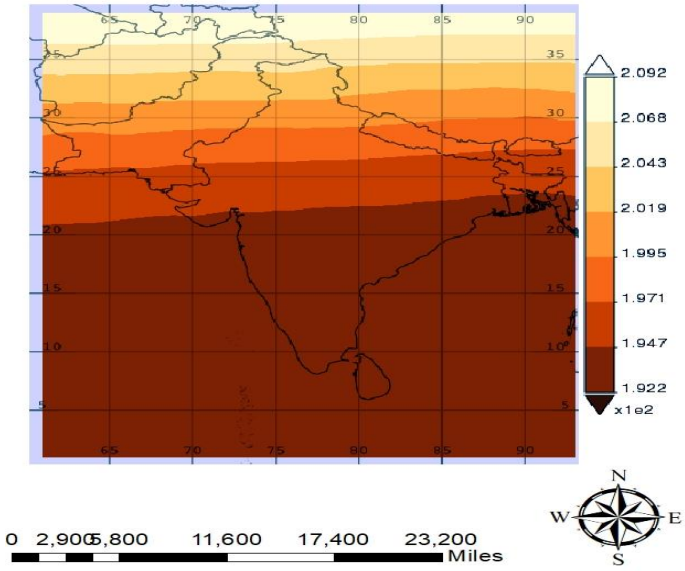

Figure 19. Map of Air temperature, average of monthly observation with spatial resolution 1 deg (Jan-1-2009 to Dec-31-2019) by AIR

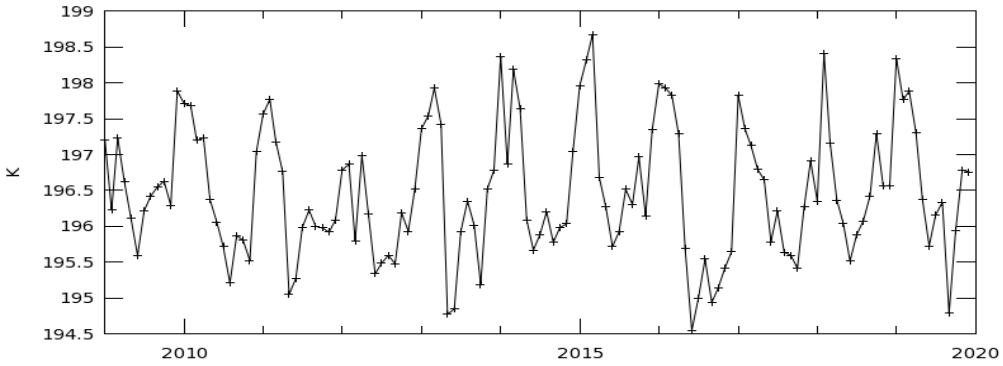

Figure 20. Temporal variation of Air temperature, average of monthly observation with spatial resolution 1 deg (Jan-1-2009 to Dec-31-2019) by AIRS

Figure 19 is showing the spatial distribution of temperature of air and Figure 20 shows temporal variation of atmospheric temperature. It works as catalyst in production of different pollutants (aerosols) already discussed in previous sections.

Conclusion.

There exists a global race to build regional economies through industrialization. This industrial revolution is responsible for addition of various toxic gasses in our environments which are dangerous for human survival and sustainable development. These toxic pollutants have become a major cause of global warming, smog and acid rain. This research shows that the CO and CO_2 causes global warming and oxides of sulfur and nitrogen cause acid rain when reacts with water droplets present in atmosphere. Therefore, efficient ways are required to handle these pollutants to save our environment for a green future. Greenery is the best way to overcome concentration of these pollutants in atmosphere.

Acknowledgement. We would like to acknowledge the profound services of NASA for providing reliable global data at Giovanni website (http://giovanni.gsfc.nasa.gov/).

Author's Contribution. I collected data from GIOVANNI and define its spatio-temporal domains, my co-author's did proof reading helped to organize data and content writing.

Conflict of interest.. There is no conflict of interest for publishing his research paper in IJIST.

Project details. NIL

REFRENCES

1. A. G. Streng, ""Tables of Ozone Properties".," Journal of Chemical Engineering Data., vol. 6, issue no. 3, pp: 431–436, 1961.

2. Brown, Geoffrey. The inaccessible earth: an integrated view to its structure and composition. Springer Science & Business Media, 2012.

3. L. Chan, L. H.Y., K. Lam and T. Wang, "Analysis of seasonal behavior of tropospheric Ozone at Hong Kong.," Atmospheric Environment, vol. 32, pp: 159-168, 1998.

4. Vignais, Paulette M., and Bernard Billoud. "Occurrence, classification, and biological function of hydrogenases: an overview." Chemical reviews, Vol 107, issue no. 10 pp: 4206-4272, 2007.

5. Iqbal, S. A., and Y. Mido. Chemistry of Air & Air Pollution. Discovery Publishing House, 2010.

6. Carvalho, M. Rosário, António Mateus, João C. Nunes, and José M. Carvalho. "Origin and chemical nature of the thermal fluids at Caldeiras da Ribeira Grande (Fogo Volcano, S. Miguel Island, Azores)." Environmental Earth Sciences 73, no. 6 (2015): 2793-2808.

7. Flannery, Tim. The weather makers: The history and future impact of climate change. Text Publishing, 2008.

8. Alastuey, A., X. Querol, S. Rodriguez, F. Plana, A. Lopez-Soler, C. Ruiz, and E. Mantilla. "Monitoring of atmospheric particulate matter around sources of secondary inorganic aerosol." Atmospheric Environment 38, no. 30 (2004): 4979-4992.

9. Torres, Omar, AapoTanskanen, Ben Veihelmann, ChangwooAhn, Remco Braak, Pawan K. Bhartia, PepijnVeefkind, and PieternelLevelt. "Aerosols and surface UV products from Ozone Monitoring Instrument observations: An overview." Journal of Geophysical Research: Atmospheres 112, no. D24 (2007).

10. Burrows, John P., Mark Weber, Michael Buchwitz, Vladimir Rozanov, Annette Ladstätter-Weißenmayer, Andreas Richter, RüdigerDeBeek et al. "The global ozone monitoring experiment (GOME): Mission concept and first scientific results." Journal of the Atmospheric Sciences 56, no. 2 (1999): 151-175.

11. Iqbal, S. A., and Y. Mido. Chemistry of Air & Air Pollution. Discovery Publishing House, 2010.

12. McAllister, Jerome W., Gunter A. Kohler, and Virtudes R. Lund. "Carbon monoxide monitoring system." U.S. Patent 4,256,694, issued March 17, 1981.

13. Dentener, F., D. Stevenson, J. Cofala, R. Mechler, M. Amann, P. Bergamaschi, F. Raes, and R. Derwent. "The impact of air pollutant and methane emission controls on tropospheric ozone and radiative forcing: CTM calculations for the period 1990-2030." (2005).

14. Madsen, Jørgen, Bjarne Schmidt Bjerg, Torben Hvelplund, Martin Riis Weisbjerg, and Peter Lund. "Methane and carbon dioxide ratio in excreted air for quantification of the methane production from ruminants." Livestock Science 129, no. 1-3 (2010): 223-227.
15. J.Allen, "Tango in the Atmosphere: Ozone and Climate Change," NASA Earth Observatory, 2004.
16. J. R. Barker, Problems and Progress in Atmospheric Chemistry, vol. 3, Advanced Series in Physical Chemistry, Ed., Singapore: World Scientific, 1995.
17. J. M. Prospero, P. Ginoux, O. Torres, S. E. Nicholson and T. E. E. Gill, "nvironmental characterization global sources of atmospheric soil dust identified with the Nimbus 7 total ozone mapping spectrometer (TOMS) absorbing aerosol product.," Rev. Geophys, vol. 40, p. 1002, 2002.
18. Shrotryia, Vijay Kumar. "An Introduction to Human Well-Being, Policy and South Asia Region." In Human Well-Being and Policy in South Asia, pp. 1-18. Springer, Cham, 2020.
19. Flannery, Tim. The weather makers: The history and future impact of climate change. Text Publishing, 2008
20. Xue, Yong, Yingjie Li, JieGuang, Xiaoye Zhang, and Jianping Guo. "Small satellite remote sensing and applications–history, current and future." International Journal of Remote Sensing 29, no. 15 (2008): 4339-4372.
21. Acker, James, RadinaSoebiyanto, Richard Kiang, and Steve Kempler. "Use of the NASA Giovanni data system for geospatial public health research: example of weather-influenza connection." ISPRS International Journal of Geo-Information 3, no. 4 (2014): 1372-1386.
22. Boersma, K. F., H. J. Eskes, J. P. Veefkind, E. J. Brinksma, R. J. Van Der A, M. Sneep, G. H. J. Van Den Oord et al. "Near-real time retrieval of tropospheric NO 2 from OMI." (2007).
23. Parkinson, Claire L. "Aqua: An Earth-observing satellite mission to examine water and other climate variables." IEEE Transactions on Geoscience and Remote Sensing 41, no. 2 (2003): 173-183.
24. Gautier, Catherine, Yang Shiren, and Mark D. Hofstadter. "AIRS/Vis near IR instrument." IEEE transactions on geoscience and remote sensing 41, no. 2 (2003): 330-342.

OPEN ACCESS International Journal of Innovations in Science & Technology

IJIST
P ISSN : 2618-1630
E ISSN : 2909-6130

Appraisal of a Running Glacier of Pakistan in Context of Geological Perspectives

Sana Yaqoob Alvi[1], Ali Abbas[2]
[1]Institute of social and cultural studies, University of the Punjab
[2] Department of Geography, University of the Punjab
Correspondence: Sana Yaqoob Alvi, Sanaalvi512@gmail.com
Citation |Alvi.S.Y, Abbas. A "Appraisal of a running glacier of Pakistan in context of geological perspectives". International Journal of Innovations in Science & Technology, Vol 03 Issue 01: pp 16-23, 2021.
Received |Jan 16, 2021; Revised | Jan 30, 2021; Accepted | Feb 08, 2021; Published | Feb 10, 2021.

Abstract

Shishper glacier is surge type glacier which gave rise to Glacier Lake Outbursts Flood (GLOF) and an ice dammed lake. The probability of GLOF events has been increased in Pakistan's mountain system due to increased temperature and irregular glacial fluctuations in northern region of Pakistan. The average rise of temperature in Pakistan is 1.04 ◦C from the year 1960 to 2014. Rising temperature is initiating the recession of glaciers over the last decade which is indicating towards the evolution of glacial lakes in Basin of Hunza River. The Shishper glacier has travelled 800m during six months and about 1400m in the next six months in the year 2018. Shishper glacier has created a danger to infrastructure of downstream of Hassanabad valley situated just below the hill. It travelled about 2.2km during 12 months. Temporal satellite imagery was used to evaluate susceptibility of GLOF events. Digital Elevation model was used to evaluate drainage patterns of Shishper glacier. Geological maps evaluated the geo-refred fault lines in the mountainous regions of Pakistan.

Keywords: Outbursts susceptibility; glacial lake; Digital Elevation model ; GLOF; Hunza River Basin

INTRODUCTION

The main incentive behind the evolution and extension of glacial lakes is the changing climate. The average rise of temperature in Pakistan is 1.04 ◦C from the year 1960 to 2019[1]. According to Pakistan Meteorological Department (PDM), the temperature raised up to 0.8 ◦C in northern areas while the rise in southern areas was observed up to 0.6 ◦C in from year 1900 to 2000 [2] which is an alarming situation. Representative Concentration Pathway(RCP)indicatedworst climatic change at global level which projects that a rise in temperature will occur up to 4.8 ◦C by the end of 21thcentury [3]. Thus, the northern areas of Pakistan aremore vulnerable to climatic change. The maximum rise in temperature was observed up to 1.79 ◦C in winter in upper Indus Basin from the year 1967 to 2005 while an annual fluctuation of 0.04 ◦C

was recorded[4].About 44.02% decline in glacial volume was recorded in the Hunza River Basin in 1989 while a decline of 34.99% was recorded in the year 2010 [5]. Rising temperature is initiating the recession of glaciers over the last decade which is indicating towards the evolution of glacial lakes in Hunza River [6].

These mountainous regions are destabilized and have become susceptible because of different anthropogenic and socio economic activities [7]. Nearly 36 out of 3044 glacial lakes were identified as critical risk [8] which cannot be estimatedby standard statistical methods. Glacial lacks are monitored and assessed temporally and spatially using remote sensing techniques, which are used to observe harsh climatic changes for the collection of data over mountains [9].

The probability of GLOFs is increased by glacier fluctuations caused by changing climate which led to the development and growth of glacial lakes. Thus, data is required for the analysis of water management for glacial lake andmanagement of GLOFs[10].

Nearly 36 glacial lakes are tantamount to flood outbursts due to high GLOF probabilityespecially, rapid climatic changes result in melting of glaciers, threatening the downstream infrastructure [11]. The status of glacial lakes is fluctuating according to the varying GLOF events. The fluctuations in these lakes may be unexpected and irregular. Surging glaciers are disastrous for downstream mountainous communities which are at a high flood risk [12].

This research was conducted to appraise the main response behind the running Shishper Glacier by incorporating local geology, hydrology and slop gradients.

Material and Methods

Study Area

This area under investigation lies within Karakoram Rangebounded bylatitudes 36◦32–37◦05N, 74◦02–75◦48E (Figure1). Hunzariver is known for the high frequency mountains and glaciers. Theseglaciers are located at 7850 m above the sea level [13].

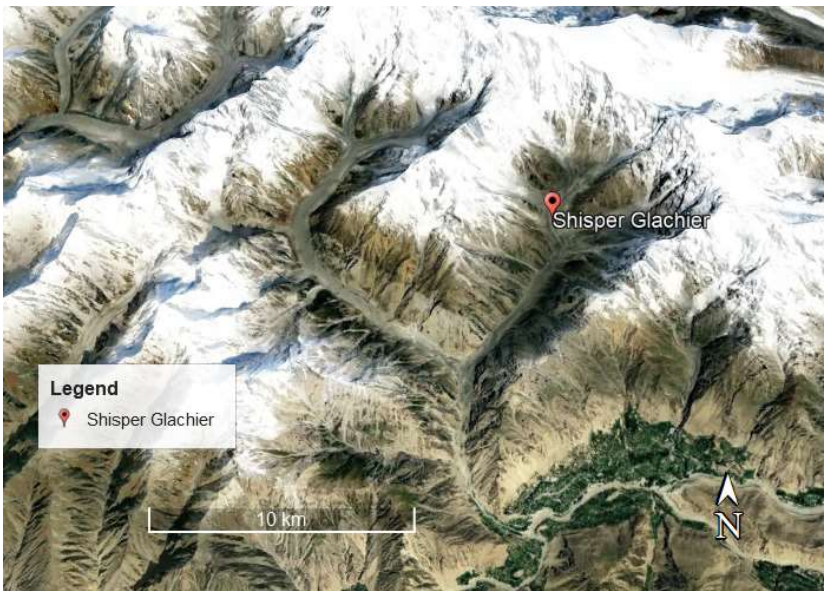

Figure 1. A 3D profile of study site.

Bedrock Geology and Tectonics

The Northern region of Karakoram exhibits complex geography which is appropriate for comprehensive study. The Reshunfault is locatedat 200 km in east with upper Hunzafault in Chitral which shows its progression along the tectonic structures located in the upper Chupurson valley [14,15,16].

The flow of methodology adopted to accomplish this research is as below,

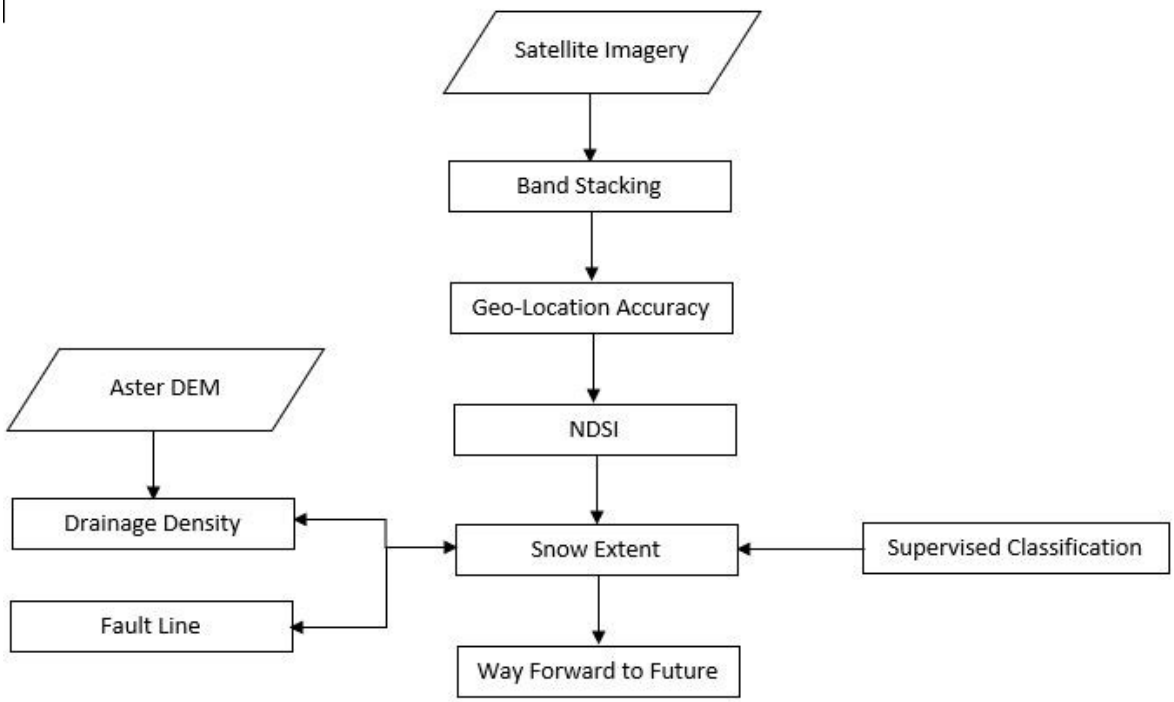

Figure 2. The flow of methodology.

Geography and Glaciers

Nearly 13,730 km^2 region is covered by Hunzariver basin which cover almost 30% of this area.Hunzariver receive penalty of water due to melting of glaciers located at highest altitude of Hunzariver in Khunjrab valley besides Kashgar of China [17]. At the middle altitude, two main streams (e.g., Misgar andChupurson) of Ziarat contributes melt-water to Hunza River followed by Shimshal stream [18]. At the lowest altitude, tributaries of the Shishper glacier cause to add melted-water into the Hunzariver. The melted-water is used by the downstream population of Pakistan for irrigation, energy production and drinking [19].

Material and Methods

The datasets and their utilization isshown in methodology flowchart.The datasets used in this research paper areof three types 1) Temporal satellite imagery 2) Digital Elevation Model (DEM) of 30m resolution of Astor and 3) Geological Map.

Satellite imagery

The satellite imagery was obtained for the months of Feb, June and December of the year 2018 and of April 2021 to monitor temporal variations in displacement of Shishper glacier. We computed spectral signatures of various existing land use features.

Digital Elevation Model (DEM).

DEM is 3D representationof surface of earth.We obtained DEM of Aster 30m from United State Geological Survey (USGS) website to compute drainage pattern. High drainage density leads to high surface deformation, which are responsible for mass movement of the surface of earth.

Geological Map.

We obtained Geological map and geo-refed it to draw fault lines beneath the study site. These fault lines are responsible for large scale surface deformation of mega structures.

Normalized Difference Snow Index (NDSI).

NDSI is the popular index used to highlight snow among other landuse. The formula to compute NDSI is as below,

NDSI = Green-SWIR/Green+SWIR

Results

Maps of glacier lakes exhibited the inconsistency of distributive features of Shishperglacier concerning the elevation. Roughly 28.23% lakes observed originated from glaciers located above 4500 m whereas altitude of 2000 to 2500 m own larger area of 5.01 km^2 locating Attabad lake which incorporate 63.8% of area of all glacial lakes.

Temporal satellite imagery determines that Shishper glacier has travelled 800m during six months and about 1400m in the next six months as shown in figure 3.The spectral signatures of various landuse features were obtained as shown in the figure 3. The NDSI was computed for cross verification of snow extent.

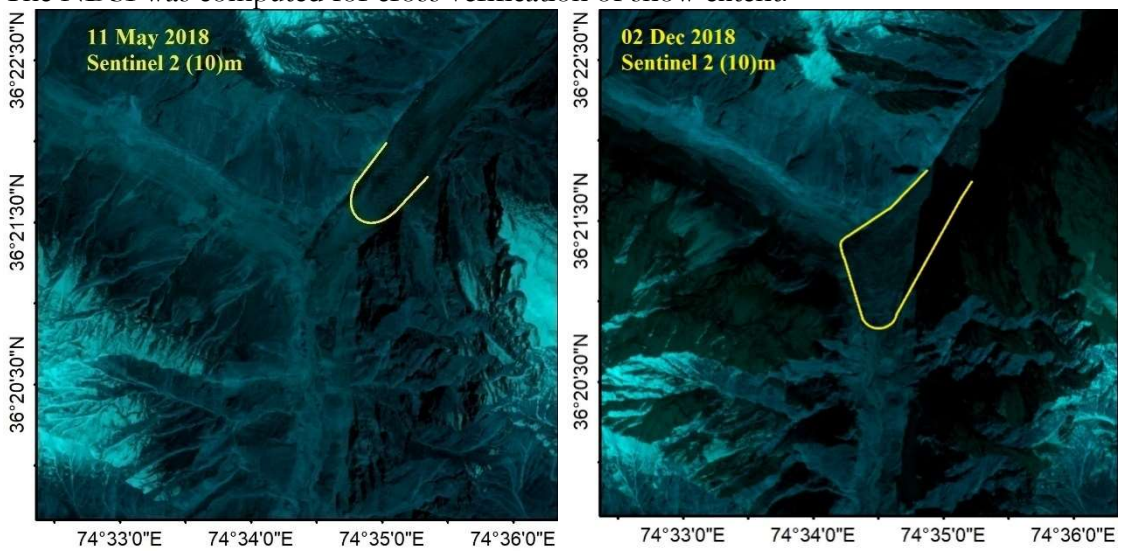

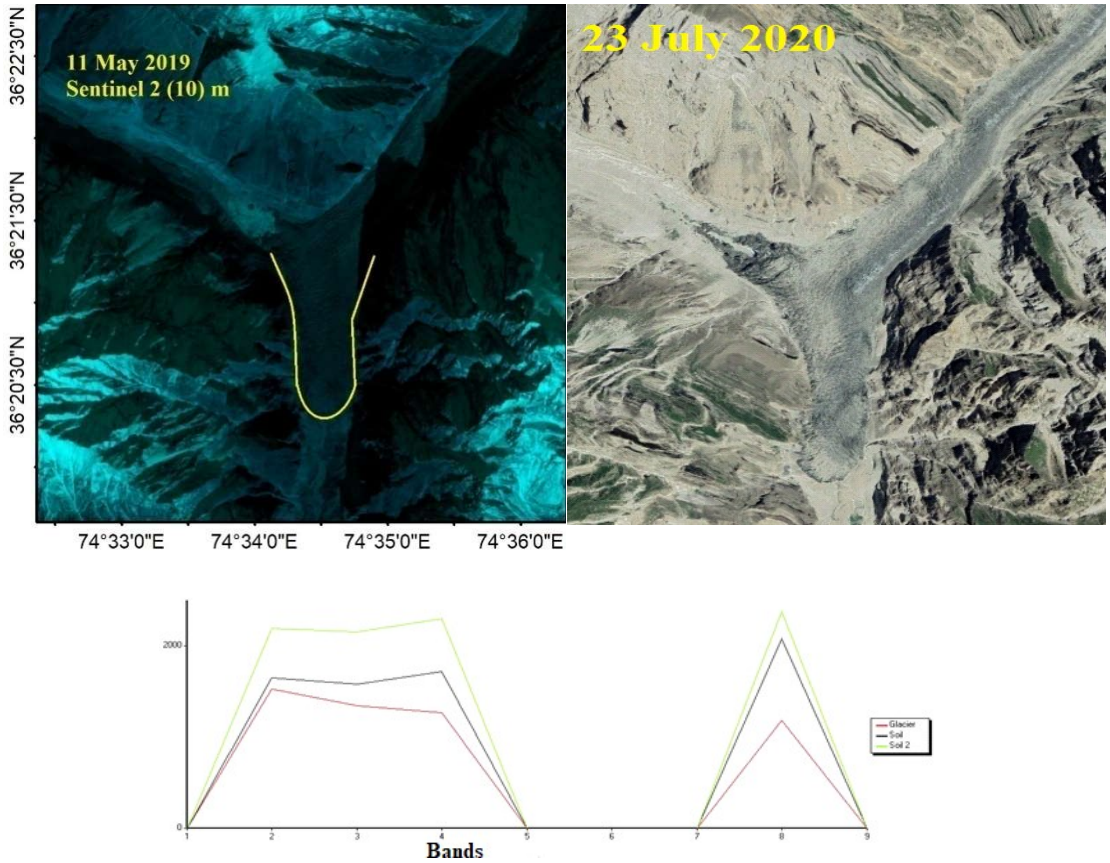

Figure 3. Spatio-temporal variation of displacement of Shisper Glacier and the spectral signature of various landuse features under observation.

The fault lines were extracted from geo-efred geological map to determine the impact of local geology on mass movement, and the results are drawn in the figure 4.

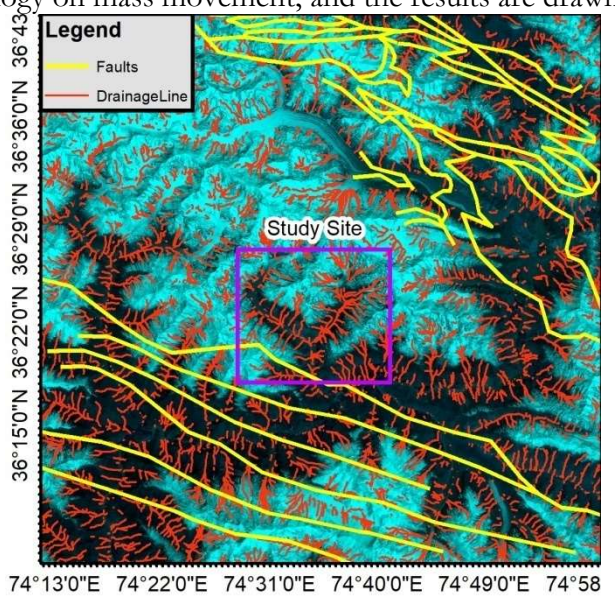

Figure 4. Integrated map of fault line map and drainage density.

The automated drainage pattern was drawn to examine the spatial distribution of drainage density as shown in the figure 4. Drainage density plays a vital role for understanding the regional tectonic setting in a better way.

Discussion

Figure 3 is showing a big mass of snow and running Shishper glacier which created a danger to infrastructure of Hassanabad situated just below the hill. It travelled about 2.2km during 12 months. There may be multiple reasons behind these movement for instance geological settings. Figure 4is showing that there is an amalgam of fault lines which is responsible for instability in terms of mass movement. The drainage density map shows that the density of streams has increased many folds where the fault lines are situated. The complex drainage points the areas where there are heavy disturbance beneath the surface of earth. Main Karakorum fault is very famous which lies underneath the study site. This fault is most probably responsible for the movement of Shishper glacier. We computed the slope factor and found that the elevation dropwas about 550m within a distance of 7km, which show that there is high slop which may be favorable for Shishper to move forward. The main reason behind stoppage of this landmass in the accumulation of snow at month in which glaciers are projected to move fast, following the previous patterns.

Way forward.

Elevation drop on the way to Shishper glacier was computed to estimate slop factor as shown in the figure 5. This slop factor is important to examine sustainable assessment in future.

Figure 5. Elevation drop on the way of Shishper

It is probable to say that the snow mass is accumulating and a pressure is increasing. Due to slop factor, once the glacier start moving, it will destroy every kind of infrastructure on its way. Therefore, it is recommended that human settlements must be displaced to a suitable place to save human lives. The activation of this glacier may be in very near future due to its position on geologically active fault zone.

Conclusions

Glacial lakes are globally developing in high mountains due to changing climate and recession of glaciers. Remote sensing techniques and satellite imagery methods were used to analyze glacial lakes in Hunzariver basin for the assessment of susceptibility of GLOF events. Temporal satellite imagery determined that Shishper glacier has travelled

800m in first six months and about 1400m in the next six months in the year 2018. Digital Elevation model was describing the factors of glacial lakes which trigger GLOF events for instance climatic changes and increasing temperature.

References

1. Ali,G.ScienceoftheTotalEnvironmentClimateChangeandAssociatedSpatialHeterogeneityofPakistan:EmpiricalEvidence Using Multidisciplinary Approach. Sci. Total Environ., 634, 95–108, **2018**. [CrossRef][PubMed]
2. Kougkoulos, I.; Cook, S.J.; Jomelli, V.; Clarke, L.; Symeonakis, E.; Dortch, J.M.; Edwards, L.A.; Merad, M. Science of the Total Environment Use of Multi-Criteria Decision Analysis to Identify Potentially Dangerous Glacial Lakes. *Sci. Total Environ. Vol 621*, pp: 1453–1466, **2018**.[CrossRef]
3. Ali,S.;Eum,H.I.;Cho,J.;Dan,L.;Khan,F.;Dairaku,K.;Shrestha,M.L.;Hwang,S.;Nasim,W.;Khan,I.A.AssessmentofClimate Extremes in Future Projections Downscaled by Multiple Statistical Downscaling Methods over Pakistan. Atmos. Res. Vol 222, pp: 114–133,**2019**.[CrossRef]
4. Khattak, M.S.; Babel, M.S.; Sharif, M. Hydro-Meteorological Trends in the Upper Indus River Basin in Pakistan. Clim. Res.Vol 46, pp: 103–119, **2011**. [CrossRef]
5. Wang, X.; Liu, Q.; Liu, S.; Wei, J.; Jiang, Z. Heterogeneity of Glacial Lake Expansion and Its Contrasting Signals with Climate Change in TarimBasin, Central Asia. Environ. Earth Sci. Vol 75, pp: 1–11, **2016**.[CrossRef]
6. Zhang, G.; Yao, T.; Xie, H.; Wang, W.; Yang, W. An Inventory of Glacial Lakes in the Third Pole Region and Their Changes in Response to Global Warming. Glob. Planet. Chang. Vol 131, pp: 148–157, **2015**. [CrossRef]
7. Cook,S.J.;Kougkoulos,I.;Edwards,L.A.;Dortch,J.;Hoffmann,D.GlacierChangeandGlacialLakeOutburstFloodRiskinthe Bolivian Andes. Cryosphere pp: 2399–2413, 2016.[CrossRef]
8. Nie, Y.; Sheng, Y.; Liu, Q.; Liu, L.; Liu, S.; Zhang, Y.; Song, C. A Regional-Scale Assessment of Himalayan Glacial Lake Changes Using Satellite Observations from 1990 to 2015 Remote Sensing of Environment A Regional-Scale Assessment of Himalayan Glacial Lake Changes Using Satellite Observations from 1990 to 2015. Remote Sens. Environ. Vol 189, pp: 1–13, 2017.[CrossRef]
9. Farooqi, A.B.; Khan, A.H.; Mir, H. Climate Change PerspectiveinPakistan. Pak. J. Meteorol. Vol2, pp: 11–21, 2005.
10. Hall, D.K.; Bayr, K.J.; Schöner, W.; Bindschadler, R.A.; Chien, J.Y.L. Consideration of the Errors Inherent in Mapping Historical Glacier Positions in Austria from the Ground and Space (1893–2001). *Remote Sens. Environ.* Vol *86*, pp:566–577, 2003. [CrossRef]
11. Jain,S.K.;Lohani,A.K.;Singh,R.D.;Chaudhary,A.;Thakural,L.N.GlacialLakesandGlacialLakeOutburstFloodinaHimalayan Basin Using Remote Sensing and GIS. *Nat. Hazards* Vol *62*, pp: 887–899, 2012.[CrossRef]
12. Hewitt K Tributary glacier surges: an exceptional concentration at Panmah glacier, Karakoram Himalaya. JGlaciol, Vol 53, issue 181, pp:181–188, 2007.
13. Iturrizaga L, Historical glacier dammed lakes and outburst floods in the Karambar valley(Hindukush-Karakoram). Geo Journal, VOL 63, issue 1–4, pp: 1–47, 2005.
14. Fang, Y.; Cheng, W.; Zhang, Y.; Wang, N.; Zhao, S.; Zhou, C.; Chen, X.; Bao, A. Changes in Inland Lakes on the Tibetan Plateau over the Past 40 Years.J. Geogr. Sci. Vol 26, pp: 415–438, 2016.[CrossRef]

15. Frey,H.;Huggel,C.;Paul,F.;Haeberli,W.Aut**omat**ed Detection of Glacier Lakes Based on Remote Sensing in View of Assessing Associated Hazard Potentials. Grazer Schriften Geogr. Raumforsch. Vol 45, pp: 261–272, 2010.
16. Huggel,C.;Kääb,A.;Salzmann,N.;Group,G.GIS-Based Modeling of Glacial Hazards and Their Interactions Using Landsat-TM and IKONOS Imagery. Nor. Geogr. Tidsskr.Nor. J. Geogr. Vol 58, pp: 61–73, 2004. [CrossRef]
17. Prakash,C.Outburst Susceptibility Assessment of Moraine-Dammed Lakesin Western Himalaya Usingan Analytic Hierarchy Process. Earth Surf. Process. Landforms Vol 2321, pp: 2306–2321, 2017.[CrossRef]
18. Aggarwal, S.; Rai, S.C.; Thakur, P.K.; Emmer, A. Geomorphology Inventory and Recently Increasing GLOF Susceptibility of Glacial Lakes in Sikkim, Eastern Himalaya. Geomorphology **Vol** 295, pp: 39–54, 2017.[CrossRef]
19. Zhu,L.;Xie,M.;Wu,Y.QuantitativeAnalysisofLakeAreaVariationsandtheInfluenceFactors from1971to2004intheNamCo Basin of the Tibetan Plateau. *Chin. Sci. Bull.* **Vol** *55*, pp: 1294–1303,2010.[CrossRef]

OPEN ACCESS International Journal of Innovations in Science & Technology

IJIST
P ISSN : 2618-1630
E ISSN : 2909-6130

A Study of Active Chaman Fault System (CFS) using SRTM DEM

Khubaib Abuzar[1],Saira Batool[2], Areeba Amer[3], Syed Amer Mahmood[4], Hania Arif[4], Bushra Talib[4], Muhammad Shahazad[6], Rana Muhammad Sohail Aslam[3]

[1]University of Sindh Jamshoro,
[2]Center For Integrated Mountain Research (CIMR), University of the Punjab, Lahore.
[3]College of Earth and Environmental Sciences (CEES), University of the Punjab, Lahore
4 Department of Space Science, University of the Punjab, Lahore
[6]Department of Technology & engineering, University of the Lahore.
[7]Department of Computer Science (PUCIT), University of Punjab.
*Corresponding Author: KhubaibAbuzar, Khubaibabuzar72@gmail.com
Citation | Abuzar. K, Batool. S, Amer. A, Mahmood. S. A, Arif. H, Talib. B, Shahazad. M, Aslam. S. M.R, "A Study of Active Chaman Fault System (CFS) using SRTM DEM". International Journal of Innovations in Science & Technology, Vol 03 Issue 01: pp 24-32, 2021.

Received |Jan 12, 2021; Revised | Jan 25, 2021; Accepted | Feb 12, 2021; Published | Feb 15, 2021.

Abstract
Chaman fault is a seismically active fault running over 850km in western region of Pakistan and Afghanistan. It is a major geological structure between Indian and Eurasian plates. Chaman fault is a strike slip fault which is slipping nearly at the rate of 10mm per year. This research includes the evaluation of lithological processes and neotectonics activity using Hypsometric Integral (HI). We calculated values of hypsometric integral using SRTM DEM with 90m spatial resolution in active region of Chaman Fault (CF) and in its locality. We analyzed different mean, minimum and maximum elevations using regular square grids and measured the degree of spatial distribution of HI using Local Indices (LI) of Spatial Autocorrelation (LISA). LISA provides auto correlation for the cluster analysis of hotspots and cold spots of HI values to discriminate uplifted and eroded regions.
Keywords: Chaman fault, LISA, DEM, Strike slip, Hypsometric integral, Neotectonics, Pakistan.

Introduction

The Chaman Fault is a seismically active sinisterly fault. It is an arrangement of geological structures that tectonically discriminates Eurasian plate from Indo-Australian plate [1]. It is the most tectonically active fault of Pakistan having almost 200km displacement in Northern region of Afghanistan. In this region the convergence occur which causes the slip

displacement of Chaman fault. The Chaman fault is the strike-slip left lateral fault which links Makran and Himalayan subduction zones [2]. These subduction zones are spatially originated by the collision of Indian and Eurasian plates. This is the largest seismically active strike slip fault. The shear zone is the most prominent strain zone located between the western alluvial and eastern meta sediment region of the fault [3].

The basin of Chaman fault is a ~80 × 20 km arc which is asymmetrical basin comprising of alluvial deposits and discontinuous spatial drainage network. The basin has developed in the response of relative uplift in Khojak Pass Mountains [4] in eastern region of fault. The southern edge of Chaman basin consists of complex erosional structures while the eastern edge of basin consists of strike slip and second order thrust fault [5].

The northern edge of Indian plate facing the Eurasian plate is vulnerable to noticeable seismic activity resulting in tectonic landmarks. These landmarks comprise of the frontal Himalayan northern arc, in the northern west of Chaman fault [6]. The two major tectonic structures of Pakistan include the Main Karakorum Thrust (MKT) and Main mantle Thrust (MMT). Thus, the western and northern regions of Pakistan are more vulnerable to the earthquakes, which reside along the Iranian, Afghan and Indian micro plates [7].

The study of distribution of earthquakes in regions having faults is significant. Thus, the main objective of this study is to investigate the seismically active segments of faults and geomorphic features hosting future earthquakes. The study reveals the geomorphic and geodic features of Chaman fault to investigate its spatial variations [8].Study of neotectonics have wide range of applications in geo sciences. The topographic features of earth comprise of erosion, tectonics and climatic changes. The geology of any region plays a vital role in the determination of variations in that region [9]. The regions comprising of homogenous rocks give rise to uniform uplift while the heterogeneous rocks are the cause of varying rates of uplift. Thus, Hypsometric Index (HI) can accurately analyse different developmental stages of geomorphic features of any region. In this study geomorphic features and remote sensing technology was used to study the tectonic characteristics of Chaman fault. The northern region of Chaman fault indicates slip rates ranging from 5.2-18.1mm per year [11].

The analyses of geomorphic features indicate the slip velocities which may cause earthquakes in future. The seismic faults are more vulnerable to floods. Electric strains can cause seismic slip which may generate earthquakes [12]. These faults exhibit sliding behavior within the depths of 10 to 15 km, during an inter-seismic period of fault having static frictional strength. Identification of spatial rates of distribution and depths of faults provides data about the seismic activity, mechanical conditions and slip of fault through seismic hazard analysis [13].

In this study, we used SRTM DEM to investigate the features of aseismic faults. The aseismic faults lie along the southern and central region of Afghanistan and Pakistan [14]. The Chaman fault lies in the neighborhood of Ghazaband fault and has exhibited notable earthquakes. The SRTM DEM also investigates the heterogeneous fault creeps along the Chaman fault. The HI is used to investigate distribution of plain areas concerning to the variations in elevation. The landform age and its characterization can also be evaluated using HI technique [15, 16]. The hypsometry index also analyzes the elevation and geometry of basin along the drainage network.

Study Area

The Chaman Fault is a seismically active major strike slip and laterally left fault which has hosted major earthquakes. This fault extends from Kharan to Kabul in northern boundary and extends toward Indian plate in western boundary. It links Makran to Himalayan convergence region. The fault gouge comprises of the volcanic rocks and limestone clasts [17]. The left lateral has moved up to 450 km along the Chaman fault. In the middle of the Chaman and BhallaDhor fault, there lies a transform fault region ranging from 30 to 60 km. This transform fault extends for nearly 975km between Garruk and Qila Abdullah in northern direction [18].

Materials And Methods

We used grid analysis to evaluate HI values for equal squares over DEMs with 90m and 30m resolution. We obtained ASTER GDEM from http://www.ersdac.or.jp/GDEM with 30m resolution. We obtained accurate data related to HI values through DEM SRTM 90m. The HI values indicate variations along lithological and tectonic boundaries [19].

Global Spatial Autocorrelation (Moran's I)

Spatial autocorrelation evaluates the distribution of HI values in different spatial patterns. The spatial statistical analysis evaluate autocorrelation in geo referenced data and spatial association. The global spatial autocorrelation tool can evaluate clustered, random and dispersed cell value. In this tool none of observations are represented by N and weight of each observation is recorded by SWM [20, 21]. Figure1. Shows the value of Moran which indicate positive and negative correlation. Its value may not be zero but it may be near to zero.

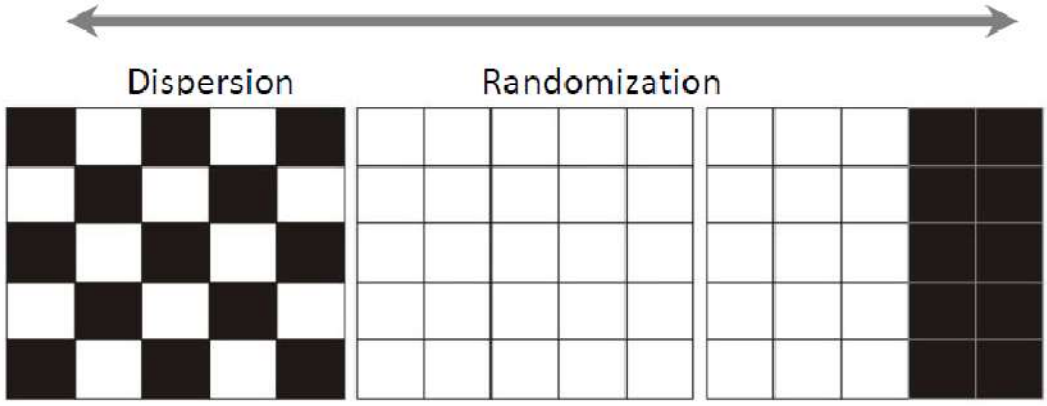

Figure1. The value of Moran remains between -1 to +1, where +1 indicates the positive correlation and -1 gives the negative correlation.

DEM resolution and HI computation

The value of HI for Chaman fault and its surrounding can be calculated using SRTM DEM with 30m and 90m resolution. The drainage channels of Hindukush are less wide than 1km so we used grid of 1 km for analysis. The grids of different sizes were used for the analysis of dependency of distribution of HI values on scale.

HI value is mainly calculated through this equation.

$$HI = \frac{H_{mean} - H_{min}}{H_{max} - H_{min}}$$

Topographic Surface roughness (TSR)

The texture of surface can be evaluated through topographic surface roughness method. This tool is quite helpful in study of terrain as it displays various geographical features which include erosion, crenulations allocation and features of landform. The ratio of surface area to plane area is known as surface coarseness which is used for the analysis of morphological structures. We computed the surface coarseness using SRTM DEM surface tools v. 2.1.254 for ArcGIS [22].

Results and Discussions

Chaman is a seismically active fault, hosting a number of Earthquakes having magnitude ranging from 7 to 8.1. According to Pakistan's geological survey, the acceleration ranged from 0.24 to 0.4 for Chaman fault system. SRTM data suggests that the four faults of Chaman face variation up to 110 km which is nearly 7.8mm per year. The SRTM DEM investigation indicates that northern region of Chaman fault is experiencing aseismic slip movement.

The results show that the northern region of Chaman fault indicates slip rates ranging from 5.2-18.1mm per year. The HI GI* Hot spots extracted through SRTM DEM are shown in Figure 2-7, the slope and TSR is mapped in Figure 8,9.

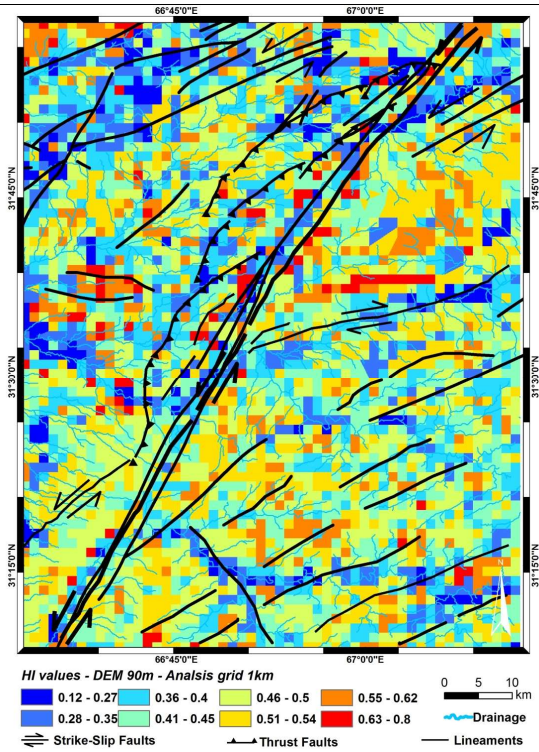

Fig. 4.1 Hi values distributions from SRTM DEM for 1 Km grid

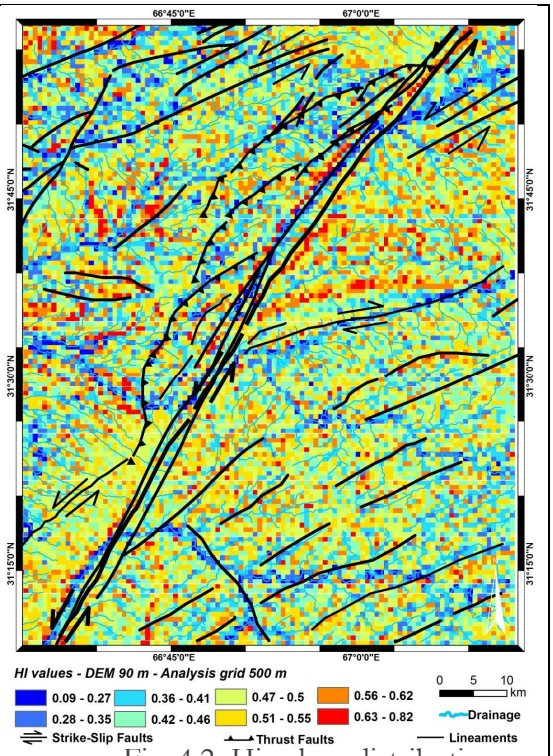

Fig. 4.2 Hi values distributions from SRTM DEM for 500 m grid

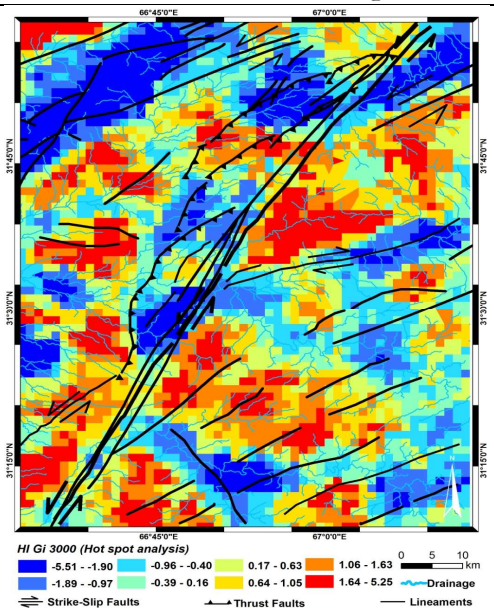

Fig. 4.3 HI GI* Hot spots and cold spots for 3000 m forn1 km

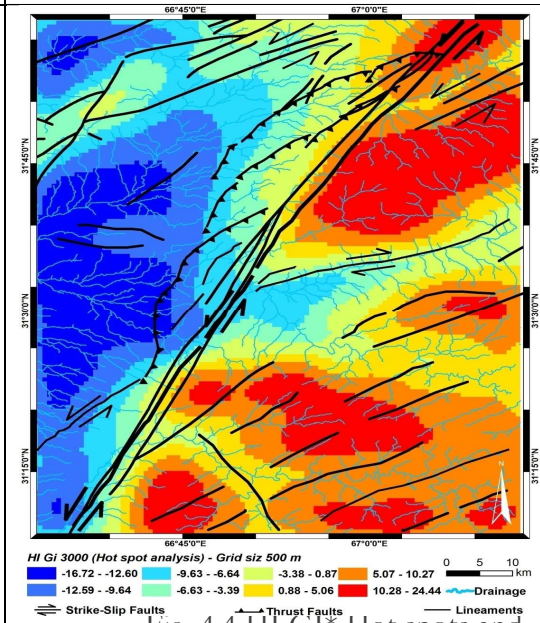

Fig. 4.4 HI GI* Hot spots and cold spots for 3000 m for 500 m.

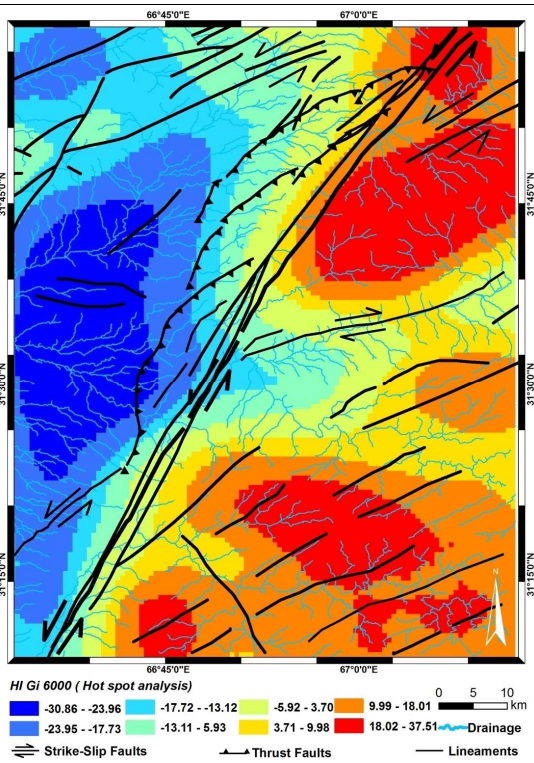

Fig. 4.5 HI GI* Hot spots and cold spots for 6000 m 500m.

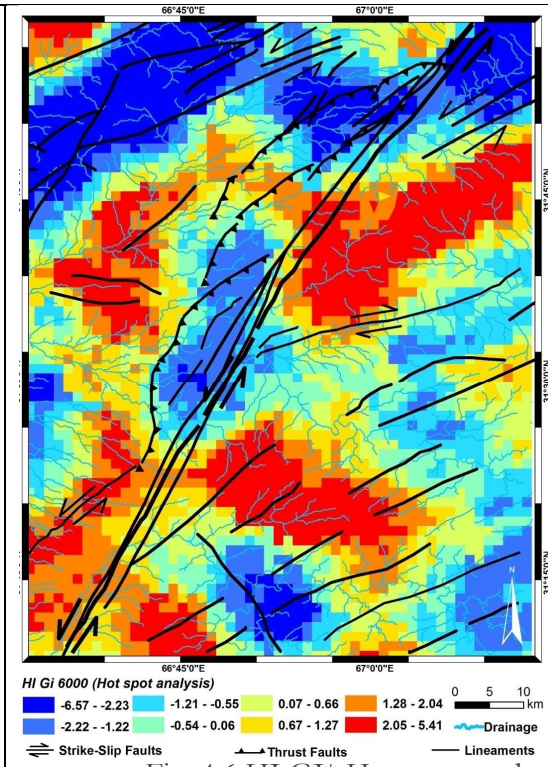

Fig. 4.6 HI GI* Hot spots and cold spots for 6000 m for 1 km.

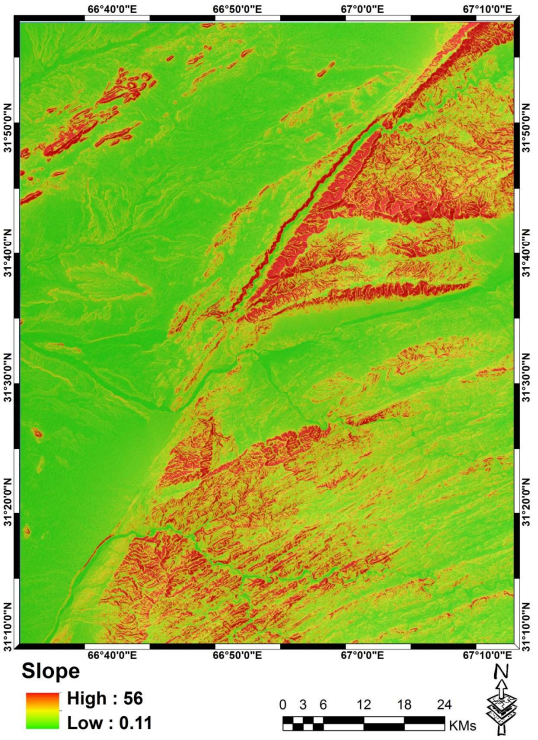

Fig. 4.7 Slope map for the study area.

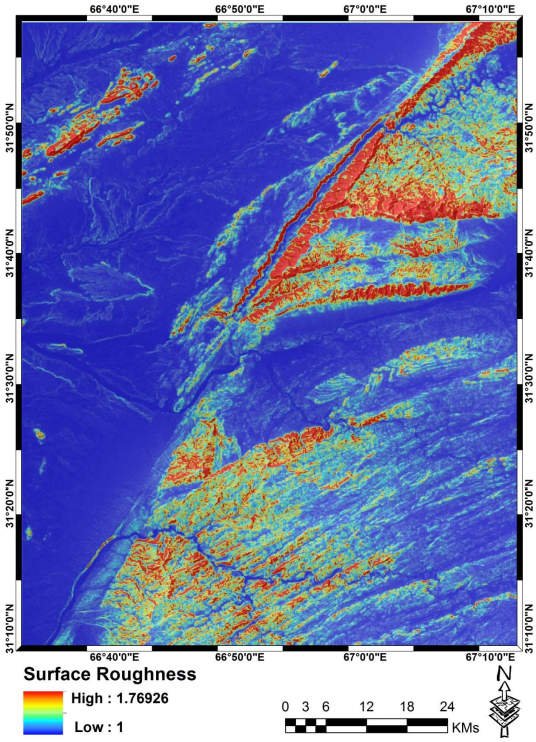

Fig. 4.8 topographic surface roughness area.

The global Moran index (GMI) statistics demonstrate that the HI-values are spatially auto-correlated and show high positive z-scores. As the investigation grid becomes coarser for the similar DEM, the z-scores reduce; indicating that the spatially disseminated autocorrelation patterns are dependent on scale.DEM spatial resolution also influences the z-scores. For SRTM data, z-scores are reduced in contrary to values from GDEM data; though, these changes are small.

The hotspot investigations made with different DEMs and the similar grid size are comparable, but when the square grid size is increased the resolution of the hot spot is also lost (e.g., the spatial resolution of hotspots for a grid size of 1 km, 2 km, and 4 km is dissimilar). As a result, we can say that GMI and Gi* investigations of HI values are scale dependent but are more robust with increasing DEM spatial resolution. The hot spots are spatially distributed along almost NE-SW–along the NE-SW oriented CF-system and adjoining regions. The CF and its plays are generally NE-SW and N-S oriented. In contrast, the general pattern of younger recent faults is being transformed from NE to the NW, cutting across the NE-trending older faults. The noticeable variation between the older NE-directing faults and the younger N to NW-trending features propose that a change in deformation style has occurred, from an preliminary stage of shortening to a more recent phase of shearing and NW-directed crustal extrusion along strike-slip fault zones. The style of broad deformation is consistent as found in the slope and topographic surface maps as well (Figures 8 and 9.)

Conclusions

Chaman fault is a seismically active fault running over 850km in western region of Pakistan and Afghanistan. We calculated values of hypsometric integral using SRTM DEM with 90m spatial resolution in active region of Chaman Fault (CF) and in its locality. The results show that the northern region of Chaman fault indicates slip rates ranging from 5.2-18.1mm per year.

The results depend upon the techniques and methods applied on Chaman fault. We calculated values of hypsometric integral using SRTM DEM with 90m spatial resolution in active region of Chaman Fault (CF) and in its locality. High and low HI values and global Moran's Index are tools used to evaluate geomorphic structures of Chaman fault and its vicinity. These tools identify and calculate the spatial patterns in datasets.

References

1. Apel, E.R., Burgmann, P., Bannerjee, and B. Nagarajan, 2006, "Geodetically constrained Indian plate motion and implications for plate boundary deformation", in American Geophysical Union, Fall Meeting 2006.
2. Abdullah, S., and V.M. Chmyriov, *Map of mineral resources of Afghanistan: Ministry of Mines and Industries of the Democratic Republic of Afghanistan*, Department of Geological and Mineral Survey, 1977.
3. Amrhein, C., and H. Reynolds, "Using the Getis statistic to explore method aggregation effects in metropolitan Toronto census data", Canadian Geographer, Vol 41, issue 2, pp : 137-149, 1997.
4. Andermann, C., and R. Gloaguen, "Estimation of erosion in tectonically active orogenies.Example from the Bhotekoshi catchment, Himalaya (Nepal)", International Journal of Remote Sensing, Vol 30, issue 12, pp; 3075-3096, 2009.
5. Anselin, L., "Local indicators of spatial association-LISA", Geographical Analysis, Vol 27, issue 2, pp: 93-115, 1995.
6. Bannert, D., Cheema, A, and A. Ahmad, "The geology of the Western Fold Felt: Structural interpretation of the Landsat-MSS Satellite Imagery". Hannover: Federal Institute of Geosciences and Natural Resources, 1992.
7. Blanchard, S.D., Rogan, J., and D.W. Woodcock, "Geomorphic Change Analysis Using ASTER and SRTM Digital Elevation Models in Central Massachusetts, USA", GIScience and Remote Sensing, Vol 47, issue 1, pp: 1-24, 2010.
8. Burtman, V., and P. Molnar, *Geological and geophysical evidence for deep subduction of continental crust beneath the Pamir*, Special Paper Geological Society of America, Vol 281, pp: 82, 1993.
9. Calkins, J., Jamiluudin, S., Bhuyan, K., and A.Hussain, "Geology and mineral resources of the chitralpartsan area, hindukush range, northern Pakistan", United States Geological Survey Paper, Vol 33, pp: 716, 1981.
10. Chen, Y.C., Sung, Q. and K.Y. Cheng, "Along-strike variations of morphotectonics features in the Western Foothills of Taiwan: Tectonic implications based on stream-gradient and hypsometric analysis", Geomorphology, Vol 56, issue 1-2, pp: 109-137, 2003.
11. Chou, Y., *Exploring Spatial Anaylsis in Geographic information systems*. Santa Fe: Onward Press, pp: 474, 1997.
12. Cliff, A. and J.K. Ord, *Spatial processes, models and applications*. London: Pion Ltd., pp: 260, 1981.

13. Doebrich, J.L., and R.R.Wahl, Geological and mineral resources map of Afghanistan, version 1, compiled by USGS, 2006.
14. Dewey, J., "The tectonic evolution of the india-eurasia collision zone", EclogaeGeologicaeHelveticae, Vol 82, issue 3, pp: 717-734, 1989.
15. Diniz-Filho, J. A. F., Bini, L. M. and Hawkins, B. A., "Spatial autocorrelation and red herrings in geographical ecology", Global Ecology and Biogeography, Vol 12, issue 1, pp: 53-64, 2003.
16. Gansser, A., *Geology of the Himalayas*, New York: Interscience, 1964.
17. Getis, A., and K. Ord, "Local spatial statistics: An overview", in *Spatial Analysis: Modelling in a GIS Environment*, Cambridge: GeoInf. Int., pp: 261-277, 1996.
18. Gloaguen, R., Marpu, P. R., and I. Niemeyer, "Automatic extraction of faults and fractal analysis from remote sensing data", Nonlinear Processes in Geophysics, Vol 14, pp: 131-138, 2007.
19. Haining, R., *Spatial data analysis in the social and environmental sciences*.Cambridge: Cambridge university press., pp: 410, 1990.
20. Hildebrand, P.R., Searle, M.P., Shakirullah, Z. A. K., and H.J. van Heijst, "Geological evolution of the Hindu Kush, NW Pakistan: Active margin to continent-continent collision zone", in *Tectonics of the Nanga Parbat syntaxis and the western Himalaya*, Geological Society, London, Special Publications Vol 170, pp: 277–293, 2000.
21. Humayon, M., Lillie, R.J. and Lawrence, R.D., "Structural interpretation of eastern Sulaimanfoldbelt and foredeep, Pakistan", Tectonics, Vol 10, issue 2, pp: 299-324, 1991.
22. Hildebrand, P.R., Noble, S.R., Searle, M.P., Waters, D. J., and R.R. Parrish, "Old origin for an active mountain range: Geology and geochronology of the eastern Hindu Kush, Pakistan", Geological Society America Bulletin, Vol 113, issue 5, pp: 625-639, 2001.

IJIST
P ISSN : 2618-1630
E ISSN : 2909-6130

Climate induced Coastline Changes: A Case Study in Togo (West Africa)

Zubair Attiq[1], Abdul Baqi[2], Ali Abbas[3]
[1]University of Lahore.
[2]Goverment Degree College Usta Muhammad, District Jaffarabad, Balochistan, Pakistan
[3]Department of Geography, University of the Punjab
* Correspondence: Zubair attiq[1] (mzubairatiq@gmail.com).

Citation | Attiq.Z, Baqi. A, Abbas.A "Climate induced Coastline Changes: A case study in Togo (West Africa)". International Journal of Innovations in Science & Technology, Vol 03 Issue 01: pp 33-42, 2021.
Received |Feb 03, 2021; Revised | Feb 15, 2021; Accepted | Feb 18, 2021; Published | Feb 20, 2021.

Abstract.

Changing climate is a global distress these days. Global warming is one of the men driven outcome of climate change which causes the glaciers to melt, shoreline regression and raises the level of sea. The regression of shoreline in Togo resulted in vandalization of human habitat and infrastructure. This research aims to monitor the coastal erosion utilizing the geospatial techniques in Togo from 1988 to 2020. The process of extraction and existence of change in shoreline is analyzed. Scientific problems regarding the precision of classification algorithms methods utilized for shoreline extraction using various satellite images are also considered. Thus, NDWI index derived from multisource satellite images were used in this research paper. The performance of Iso Cluster Unsupervised Classification, Otsu threshold segmentation and Sup- port Vector Machine (SVM) Supervised Classification techniques are monitored for the shoreline extraction. This study also takes into account the topographic morphology including non-linear and linear coastal surfaces. The rate of change of shoreline was estimated through the statistical linear regression method (LRR). The results demonstrated that the SVM Supervised Classification method worked accurately for topographic morphology than other methods.

Keywords:
Landsat Images, Coastal Erosion, Remote Sensing, NDWI, Shoreline, Sentinel Images, SVM

Introduction

The changing climate is now an active area of research because of its adverse effects globally. Global warming is one of the outcomes of climate change which results in melting of glaciers, regression of shoreline and rising sea levels. Shoreline is actually the line where land and sea meets [1]. The shoreline regression results in coastal erosion causing destruction of natural ecosystem, human habitat and the socio economic infrastructure [2].

One of the consequences of global warming is coastal erosion and increased induction. Increased global temperature has caused the reduction of ice caps which in turned has raised the level of oceans causing ocean expansion and changing wind patterns. Consequently, it results in coastal flooding and rapid regression of coastline [4, 5, 6].

Coastal regions or shorelines constitute less than 20% of surface of earth. Coastal regions host nearly 45% of population for agriculture, transportation and fishing [7]. Shorelines are one of the major energy sources utilizing tides and waves. These anthropogenic activities have posed a threat to coastlines by raising the probability of coastal erosion and shoreline regression [8].

Climate change has affected 70% of the world's coastal regions raising the risks of flood outbursts. Moreover this flooding has affected more than 200million people around the globe. Population increase and infrastructure development has raised the need of monitoring and assessment of coastal regions. Moreover effective management and planning is required for coastline development [9].

Shoreline is primary benchmark for the measurement of any kind of climate changes. Anthropogenic activities as well as natural activities cause changes in shoreline. Industrial and residential area development has caused massive changes in shorelines. Shorelines are globally being eroded due to extensive tides and storms [10].

Moreover the extensive flooding which results in extensive sediment supply to coastal regions causes erosion and disrupts the sediment transport system. The phenomena of coastal erosion severely affected the West African coast but Togolese coast is the main concern of this study. The Togolese coast has to face challenges including coastal erosion and urban expansion because of its configuration.

Konko *et al.* (2018) [2] observed that the Togo coast shoreline has experienced recession which ranges from 1.66 to 5.25 m per year while urbanization has increased up to 7.84 ha per year. These average ranges predicted that the 82.724 inhabitants of the local population are at a continual risk of inundation caused by regression of shoreline which might affect 7% or more surface area until 2070s. The induction near the beach could vandalize the infrastructure and rural exodus phenomena.

The Togolese coast is monitored to plan and define hazard zones and to predict erosion. This research paper focuses on western Togolese coast utilizing remote sensing techniques. Remote sensing technique is an accurate tool to obtain reliable information regarding shoreline. The landscape features are monitored and discriminated utilizing the preferred means which include satellite images.

The Normalized difference water index (NDWI) along modified normalized difference water index is developed to enhance the discrimination of terrestrial and aquatic zones of coastal areas using various methods of water index derived from satellite imagery.

The classification algorithms utilized for the shoreline extraction from water index has major scientific concerns regarding precision regardless that the discrimination of aquatic and terrestrial zones can be done through satellite images.

Issues related to the extraction of shoreline can be resolved using reliable tools such as image processing techniques. Some other methods including Iterative Self Organized Data Analysis (ISODATA) [11],Support Vector Ma- chine (SVM) [2] [12], thresholding and morphological filtering [13], ob- ject-oriented fuzzy classification approaches [14], Random

forest method [15], genetic algorithm based methods [16] and mean-shift segmentation [17] have been proposed for extraction of shoreline.

This research paper focuses on assessment of performance of different methods for the shoreline extraction on topographic surfaces and on the shoreline kinematics from the year 2009 to 2020.

Materials and Methods

Study Area

The study area Togo lies in West Africa bounded by Ghana. The area under study is characterized by subequatorial climate having four seasons including a dry, a rainy, a short dry and a short rainy. This area contains irregular precipitation at the rate of 1000 to 1400 mm/year. The mean temperature is usually high, about 27°C. Togo covers nearly 57000km^2 area having population of about 8 million people.

Data Used

The required data for this study was obtained from Sentinel (https://sentinel.esa.int/) and Landsat (https://landsat.usgs.gov/) platform.

Figure 1. Map of Togolese Coast West Africa for the year 2020.

Satellite imagery

The satellite images come from different sensors, including Enhanced Thematic Mapper Plus (ETM+), including Thematic Mapper (TM), and Multi Spectral Instrument (MSI) were used to obtain satellite images. The image breakdowns are as follows: ETM+ image of 13 December 2009 at 09:59:54 am, TM image of 12 February 2019 at 09:34:08 am, MSI image of 04 January 2020 at 11:18:13 am. The dates were chosen in the long dry season

in order to use images that were sensed in similar conditions and similar time for a coherent data analysis [18].

Optical images

ENVI software was used to preprocess the acquired optical images. The images are first geo refrenced with the help JICA topographic data and GPS field surveys in accordance with the World Geodetic System the UTM projection. Subsequently the images are processed for radiometric and geometric correction and then for re sampling. The atmospheric effects were reduced using radiometric correction, while the geometric correction removed the geometric distortion [19].

NDWI technology

In order to enhance the terrestrial and aquatic zone discrimination various water index methods have been developed including modified normalized difference water index and Normalized difference water index. In this research NDWI is used due to its accuracy, convenience and efficiency [20].

Shoreline Extraction Methods

The line joining land and sea is called the shoreline [20]. The shoreline is basically line connecting a sea with land. Changes on shoreline can be detected using various methods including Image enhancement which processes satellite images, write function memory insertion, manual method and density. Manual method, write function memory insertion, density slice using single or multiple bands and multi-spectral classification, image enhancement, Multi-date data classification, Images digitization, and comparison of two independent land cover classifications and various other methods are used for detection of satellite images and shoreline extraction. [21] [22] [23] [24] [25]. The shoreline has also been extracted automatically with satellite images various algorithms used for processing of images including segmentation, pre and post segmentation.

Three distinct methods are more accurate and commonly used for shoreline extraction on NDWI indices including Otsu threshold segmentation, SVM su-pervised Classification methods and Iso Cluster Unsupervised Classification.

Otsu Threshold Segmentation Method

Ostu proposed a dynamic method for the partition of input raster images into water regions and homogeneous land with by reducing intra class variance. The method is known as Otsu's method.

The Otsu threshold segmentation method is the most referenced method which provides dynamic variety of thresholds on the basis of different regions in different sectors. It automatically sets the value in accordance to the local features for the achievement of a good partition between sea water and land. For the calculation of thresholding level value it highly depends upon the discriminate analysis which utilizes the cumulative moments recorded in first order of the histogram.

Iso Cluster Unsupervised Classification Method

The aquatic and terrestrial environments are separated using the Iso Cluster Unsupervised Classification method. The migrating means technique is also used as a tool for modified iterative optimization clustering procedure in the Iso Cluster Unsupervised Classification. The cells are separated into user specified number having distinct uni modal

groups using the algorithm in the multidimensional space of the input bands. This method is mostly used for unsupervised classification.

The SVM Supervised Classification Method

The aquatic and terrestrial areas are also separated using SVM Supervised Classification method. It is a statistical non parametric technique which is in general used to maximize the margins and to separate observations on the basis of search for hyper-plane. The original formulation of the algorithm was dev3eloped by Vapnik (1982) [37]. SVM also minimizes the risk of error during classification and it has high performance during separation of pixels.

Shoreline Kinematics

Shoreline kinematics provides better knowledge of consequences of coastal erosion phenomenon on human habitats.

Figure 2. Map of coast subdivided into seven sectors on sentinel-2 Satellite image.

Results and Discussions

Coastal erosion due to anthropogenic activities has reached at an alarming position in Togo coast of West Africa. Aneho and Lome are the two major cities at higher risk of erosion and accretion. The changing wind patterns and tidal waves have eroded nearly 5-10 meters coastline per year.

In Togo the coastal erosion was intervened through the construction of autonomous deep sea port of Lome in the year 1968. This port can accommodate nearly nine meter depth requiring cargo ships. The process of sediment accumulation has been disrupted due to the construction of this port. Thus, this caused a loss of beaches through erosion. The construction of port effected the direction of currents which triggered sand drift off the shoreline.

Figure 3. Lome Sea port constructed at the Togolese coast.

The average rate of erosion in the region surrounding the port is nearly 3 meters per year. The figure 4 shows the regression of shoreline for the year 2009 and 2019. LRR method is used for extraction of shoreline changes for the years 2009 and 2019. The southwest of the Togolese coast show average rate of erosion ranging from 2.49 to 5.07 m/year for the shoreline kinematics.

Figure 4. Shoreline regression for the years 2009 and 2019

Figure 5. Division of Togo coastline into sections

For the better understanding of rate of erosion on the coastline of Togo, it is divided into seven sectors through shoreline kinematics. The average rate of erosion per year in these sectors is given in the table below.

Table 1. The average rate of erosion per year in these sectors

Sectors Low value (meter/year)	**a** −3.88	**b** -3.49	**c** +1.85	d −4.16	**e** −6.64	**f** −5.46	**g** −6.35
High value (meter/year)	-1.1	-1.01	+2.18	−1.84	−1.66	−2.8	−3.78
Average value	-2.49	-2.25	+2.06	−3.00	−4.15	−4.13	−5.07

The average rate of erosion is 3.00 m/year, 4.15 m/year and 4.13 m/year for d, e and f sectors respectively. The sector b records both erosion and an accretion phenomenon as the asphalt road is close to the sea which causes erosion in sector b. The sector d which is port zone indicated accretion phenomena.

Conclusions

The coastal region of Togo is monitored from 1988 to 2019 in this research paper to investigate erosion phenomena. In this study Iso Cluster Unsupervised Classification method, Otsu threshold segmentation method, and SVM Supervised Classification methods are assessed to analyze the performance for the shoreline extraction from NDWI indices on both non linear and linear surfaces. This research also takes into account the kinematics of shoreline.

According to results the SVM Supervised Classification method performed accurately on linear and non-linear coastal surface as compared to the other methods. The southwest of the Togolese coast show average rate of erosion ranging from 2.49 to 5.07 m/year for the shoreline kinematics. Sector a showed the lowest rate of erosion.

Conflicts of Interest

The authors declare no conflicts of interest regarding the publication of this paper.

Project detail. Nil

References

1. Deng, H.J., Chen, Y.N., Shi, X., Li, W.H., Wang, H.J., Zhang, S.H. and Fang, G.H. Dynamics of Temperature and Precipitation Extremes and Their Spatial Variation in the Arid Region of Northwest China. *Atmospheric Research*, 138, 346-355, 2014.
2. Konko, Y., Bagaram, B., Julien, F., Akpamou, K.G. and Kokou, K. Multi- temporal Analysis of Coastal Erosion Based on Multisource Satellite Images in the South of the Mono Transboundary Biosphere Reserve in Togo (West Africa). *Open Access Library Journal*, 5, 2018.
3. Stanchev, H., Young, R. and Stancheva, M. (2013) Integrating GIS and High Reso- lution Orthophoto Images for the Development of a Geomorphic Shoreline Classi- fication and Risk Assessment: A Case Study of Cliff/Bluff Erosion along the Bulga- rian Coast. *Journal of Coastal Conservation*, 17, 719-728, 2013.
4. Yang, B., Hwang, C. and Cordell, H.K. Use of LiDAR Shoreline Extraction for Analyzing Revetment Rock Beach Protection: A Case Study of Jekyll Island State Park, USA. *Ocean & Coastal Management*, 69, 2012.
5. Bayram, B., Seker, D.Z., Acar, U., Yuksel, Y., Guner, A.H.A. and Cetin, I. An Integrated Approach to Temporal Monitoring of the Shoreline and Basin of Terkos Lake. *Journal of Coastal Research*, 29, 1427-1435, 2013.
6. Djagoua, M., Bakayoko, F., Kouadio, M.J., Kassi, A.J.B. and Mobio, A.B.H. Cartography of Coastal Dynamics in Grand-Lahou: Tool Use "Digital Shoreline Analysis System (Dsas)". *European Scientific Journal*, 12, 327-335, 2016.

7. Blivi, A. and Adjoussi, P. La cinématique du trait de côte du Togo vue par télédétection. *Geo-Eco-Trop*, 28, 27-38, 2004.
8. Maiti, S. and Bhattacharya, A.K. Shoreline Change Analysis and Its Applica- tion to Prediction: A Remote Sensing and Statistics Based Approach. *Marine Geol- ogy*, 257, 11-23, 2009.
9. Atsri, H.K., Konko, Y., Cuni-Sanchez, A., Abotsi, K.E. and Kokou, K. Changes in the West African Forest-Savanna Mosaic, Insights from Central *PLoS ONE*, 13, 2018.
10. Konko, Contribution of Remote Sensing and GIS to the Integrated Man- agement of Community Forest Resources in the Bas-Mono Valley (South-East Togo), 2016.
11. Master's Thesis, Post University Regional School of Integrated Management of Trop- ical Forests and Territories, Kinshasa, Democratic Republic of Congo.
12. Kalkan, K., Bayram, B., Maktav, D. and Sunar, F. Comparison of SVM and Object Based Classification Methods for Shoreline *ISPRS Conference on Serving Society with Geoinformatics*, *Antalya-Turkey. ISPRS International Archives of the Photogrammetry*, *Remote Sensing and Spatial Information Sciences*, Volume XL-7/W2, 125-127, 2013.
13. Guariglia, A., Buonamassa, A., Losurdo, A., Saladino, R., Trivigno, M.L. and Zac- cagnino, A. A Multisource Approach for Shoreline Mapping and Identifica- tion of the Shoreline Changes. *Annals of Geophysics*, 49, 295-304, 2006.
14. Pardo-Pascual, J.E., Almonacid-Caballer, J., Ruiz, L.A. and Palomar Vázquez, J. (2012) Automatic Extraction of Shorelines from Landsat TM and ETM+ Mul- ti-Temporal Images with Subpixel *Remote Sensing of Environment*, 123, 1-11, 2012.
15. Demir, N., Oy, S., Erdem, F., Şeker, D.Z. and Bayram, B. (2017) Integrated Shore- line Extraction Approach with Use of Rasat MS and SENTINEL-1A SAR Images. *ISPRS Annals of the Photogrammetry*, *Remote Sensing and Spatial Information Sciences*, 4, 2017.
16. Bayram, B., Avsar, E.Ö., Seker, D.Z., Kayi, A., Erdogan, M., Eker, O., Janpaule, and Çatal, R.H. The Role of National and International Geospatial Data Sources in Coastal Zone Management. *Fresenius Environmental Bulletin*, 26, 383-391, 2017.
17. Wu, H., Liu, C., Zhang, Y. and Sun, W. Water Feature Extraction from Aeri- al-Image Fused with Airborne LIDAR *IEEE Urban Remote Sensing Event*, Shanghai, 20-22 May 2009, 1-7, 2009.
18. Yousef, A. and Iftekharuddin, K. (2014) Shoreline Extraction from the Fusion of LiDAR DEM Data and Aerial Images Using Mutual Information and Genetic Algo- 2014 *International Joint Conference on Neural Networks* (*IJCNN*), Beijing, 1007-1014, 2014.
19. UNESCO (2017) Biosphere Reserves.
20. Konko, Y., Rudant, J.P., Akpamou, G.K., Noumonvi, K.D. and Kokou, K. Spatio-Temporal Distribution of Southeastern Community Forests in Togo (West Africa). *Journal of Geoscience and Environment Protection*, 6, 51-65, 2018.
21. Nimon, P., Issaou, L., Konko, Y. and Kokou, K. Spatio-Temporal Patterns of Rainfall Variability for Wet Season over Togo in West *Open Access Library Journal*, 7, 2020.
22. Wang, X., Liu, Y., Ling, F., Liu, and Fang, F. Spatio-Temporal Change De- tection of Ningbo Shoreline Using Landsat Time-Series Images during 1976-2015. *International Journal of Geo-Information*, 6, 68, 2017.
23. Mcfeeters, S.K. The Use of the Normalized Difference Water Index (NDWI) in the Delineation of Open Water *International Journal of Remote Sens- ing*, 17, 1425-1432, 1996.

24. Mas, J.F. Monitoring Land-Cover Changes: A Comparison of Change Detection Techniques. *International Journal of Remote Sensing*, 20, 139-152, 1999.

OPEN ACCESS International Journal of Innovations in Science & Technology

IJIST
P ISSN : 2618-1630
E ISSN : 2909-6130

SRTM DEM based Neotectonics from Non-Linear Analysis: A Paradigm through Fractal Analysis

Areeba Amer[1], Syed Amer Mahmood[2], Amer Masood[3],Saira Batool[4], Hania Arif[5], Bushra Talib[5], Muhammad Shahazad[6], Rana Muhammad Sohail Aslam[7]

1,,3,4Center For Integrated Mountain Research (CIMR), University of the Punjab, Lahore.

2,7 Department of Space Science, University of the Punjab, Lahore.

4,5College of Earth and Environmental Sciences (CEES), University of the Punjab, Lahore

5Department of Technology & engineering, University of the Lahore.

6 Department of Computer Science (PUCIT), University of Punjab

* Correspondence: AreebaAmer(areebaamer001@gmail.com)

Citation | Amer. A,Mahood. S. M,Masood.A, Batool.S, Arif. H, Talib. B, Shahzad. M, Aslam. S. R.M "SRTM DEM based Neotectonics from Non-Linear Analysis: A Paradigm through Fractal Analysis". International Journal of Innovations in Science & Technology, Vol 03 Issue 01: pp 43-51, 2021.

Received |Feb 08, 2021; Revised | Feb 22, 2021; Accepted | Feb 25, 2021; Published | Feb 28, 2021.

Abstract

Neotectonics amend the river base and causes landscape erosion. This study explores the DEM based differentiation of neotectonics in the northern regions of Pakistan. This method involves vertical and non-linear dissection base on digital evaluation method. This study uses Gliding Box Technique (GBM and GBT) and Box Counting method to evaluate Lacunarity (LA), Succolarity (SA) or 3-Fractals, and Fractal Dimensions (FD). 3-fractals are an attribute used for the recognition of spatial patterns, specifically to compute and differentiate natural textures including natural patterns. This study also investigates vertical dissection using DEM SRTM having spatial resolution of 90m. DEM SRTM measures surface area, plane area as well as the surface ratio. The vertical areas are investigated to make dissection maps and to identify the affects of neotectonics on the roughness of surface. Low value of surface roughness indicates flattened drainage basins and inclination of slope. The Raikot Fault shows higher values of surface roughness towards NE- SW. The surface roughness is mapped to recognize relative uplifts, uneven regions, depressions and pits. Analysis through non-linear method identifies the regions affected by neotectonics activity. Tectonics activity causes deformation and instability in drainage networks.

Keywords: surface roughness, Gliding Box Technique, Fractal Dimension, SRTM DEM, Succolarity.

Introduction

The current topography of Gilgit-Baltistan is a consequence of continuous climatic changes and tectonic activity. Digital evaluation model is used to analyze spatial distribution patterns

of drainage network. This study deals with the fractal analyses of drainage networks. The fractals are self-identical complex objects which can be reduced to small size parts identical to the whole [1]. In nature, fractals occur in form of branches of trees, patterns of drainage network, river system and human circulatory system. The developing patterns of fractals can be explained through physical and geological activity. The fractal dimension analysis has wide applications in the field of forestry, food research, landscape ecology, tectonic geomorphology and information technology [2]. Figure 1 and 2. Shows the regional tectonics and self similar fractal objects respectively.

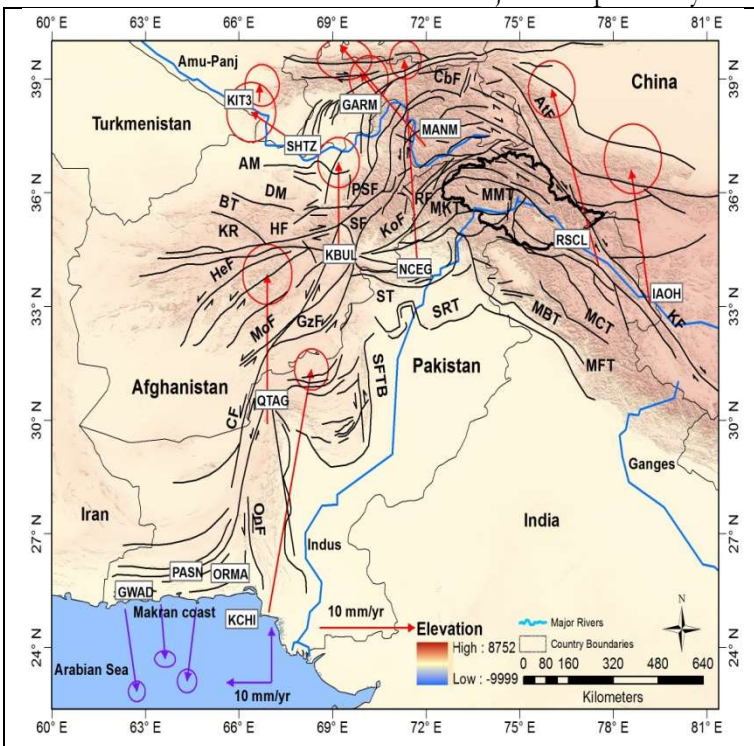

Figure.1 Regional tectonic map showing location of Gilgit Baltistan region

Figure. 2: Examples of self-similar natural fractal objects.

The main objective behind these methods is to recognize instability and variations in natural spatial patterns. Geomorphologically, asymmetrical, linear and spatial drainage patterns show the instabilities caused by geological processes. Active deformations of surface can be studied by examining the stream patterns. The deformation due to tectonic activity adjusts the spatial drainage patterns into linear configuration [3].

Lacunarity is a method used to represent the stream network in form of texture. This method accurately differentiates patterns having corresponding values of fractal dimension. The LA monitors varying self-identical conduct of fractals and its low value indicates low activity [4]. The Secularity monitors the instabilities of spatial drainage patterns. Secularity method monitors the black and white imagery perpendicularly and prospectively to monitor the infiltration capability [5]. The succolarity method determines the common rotator method of spatial drainage patterns. Its high value indicates highly deformed regions. The objective of this paper is to identify and interpret data of natural drainage networks [6].

Data and method

SRTM with 90m resolution was used to extract drainage patterns using black and white imagery. Neotectonics strongly impact surface deformation and development of landscape due to which streams display strained and linear pattern [7]. Fractal box counting technique was used in this research to display complex drainage patterns. But the fractal dimension is important to display interpretation of spatial patterns. Thus, to interpret drainage networks SA and LA methods are utilized [8].

Fractal Dimension and Box Counting Method

Fractal objects are uniform and unvarying entities. The fractal entities are self identical and homogenous objects used for determination of geomorphic indices [9]. The drainage network displays fractal like homogenous properties. Fractal dimensions determine the segmentation and deviation extent of spatial drainage patterns. This study determines the fractal dimension of Hunza, Indus and Gilgit River and computes drainage network for Gilgit-Baltistan [10]. Fractal dimensions can be computed using Box Counting method using binary pictures of variable sizes that adds up the total drainage pixels lying in a box. The square size "s" and the number of pertinent boxes "N(s)"are summed in a grid. Equation 1 shows the computation of FD:

Equation.1

$$FD = \lim_{s \to 0} \frac{\log N(s)}{\log(1/s)}$$

The total number of boxes is given by N(s) and "s" represents the size of the box side (Figure 3). The FD is represented by the slope regression of the natural log (ln) graph of total number of boxes and 1/s. The ramp color was used in FD spatial distribution map to recognize low value of FD. Generally, fractal values of spatial distribution patterns display linear images of spatial distribution pattern. Figure 3. Shows the value of FD up to 1 displays high linearization of stream networks.

Lacunarity and Gliding Box Technique (GBT)

The lacunarity is a method used to investigate varying behavior of fractal objects. The lacunarity accurately analyzes the distribution of spatial drainage networks and gaps among entities of a network [11]. The lacunarity method can also differentiate the contrary patterns of drainage network having similar fractal values [12]. The Gliding Box Technique (GBT) computes Lacunarity. (Equation.2)

Equation.2

$$\Lambda(r) = \frac{\sum_{r=1}^{N} s^2 P(s,r)}{\left[\sum_{r=1}^{N} sP(s,r)\right]^2}$$

The homogenous fractal objects have low value of Lacunarity while heterogeneous fractal objects have high Lacunarity value. The high LA values indicate distorted drainage patterns while low LA values indicates low tectonic activity. LA values higher than 2.5 indicates sever deformation.

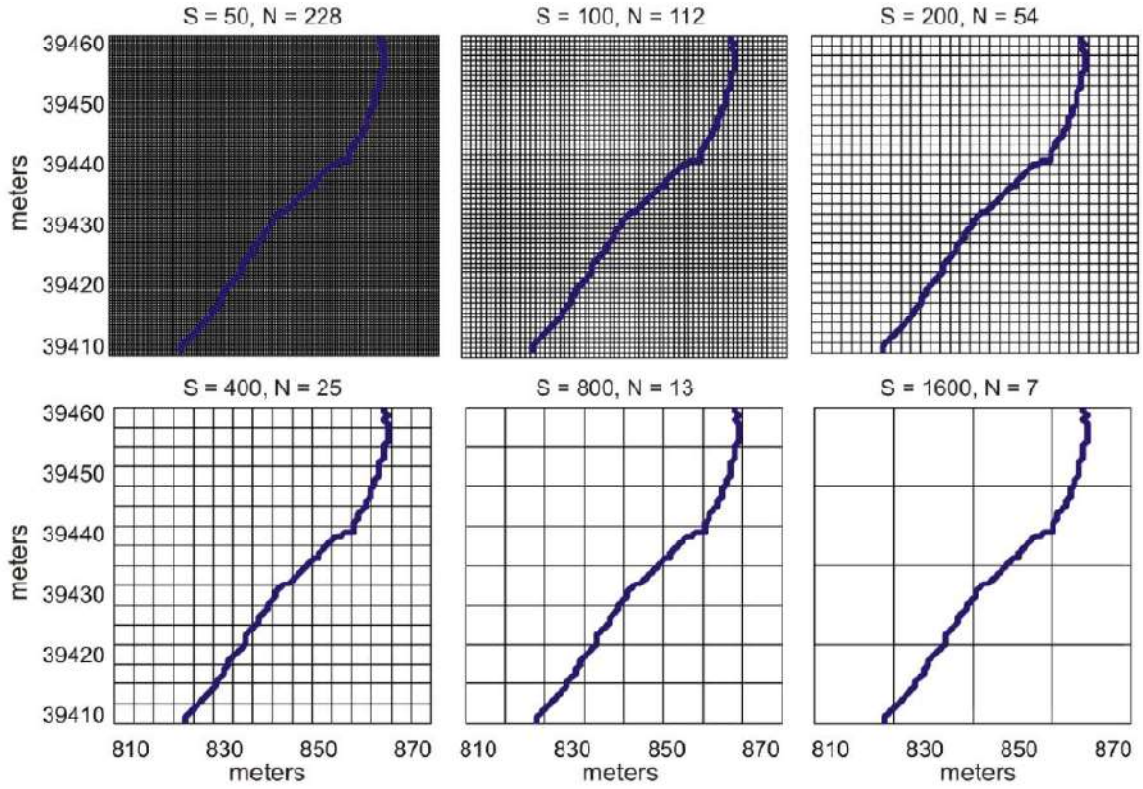

Figure 3. Calculation of Fractal Dimension (FD) by using Box counting method.

Succolarity fractal

The Succolarity method is used to calculate percolation capability of binary images. The image which is analyzed provides direction of more images.

Equation.3

$$\sigma(dir) = \frac{\sum_{k=1}^{n} NP(k).PR(pc,k)}{\sum_{k=1}^{n} PR(pc.k)}$$

Equation. 4

$$\bar{\sigma} = \frac{\sigma(T2B) + \sigma(B2T) + \sigma(L2R) + \sigma(R2L)}{4}$$

Equation. 5

$$\bar{\sigma} = \frac{\sigma(0^0) + \sigma(90^0) + \sigma(180^0) + \sigma(270^0)}{4}$$

The SA value ranging from 0 to 1 is catogrized as < less than 0.5 is low, 0.5 to 0.75 is medium and greater than 0.75 is high SA value. High Succolarity value represents distant drainage and indicates tectonic activity [13, 14, 15]. It also displays regions of active deformation due to impenetrable masses and empty gaps. Figure 4. Indicates flooded scenarios through blue boxes.

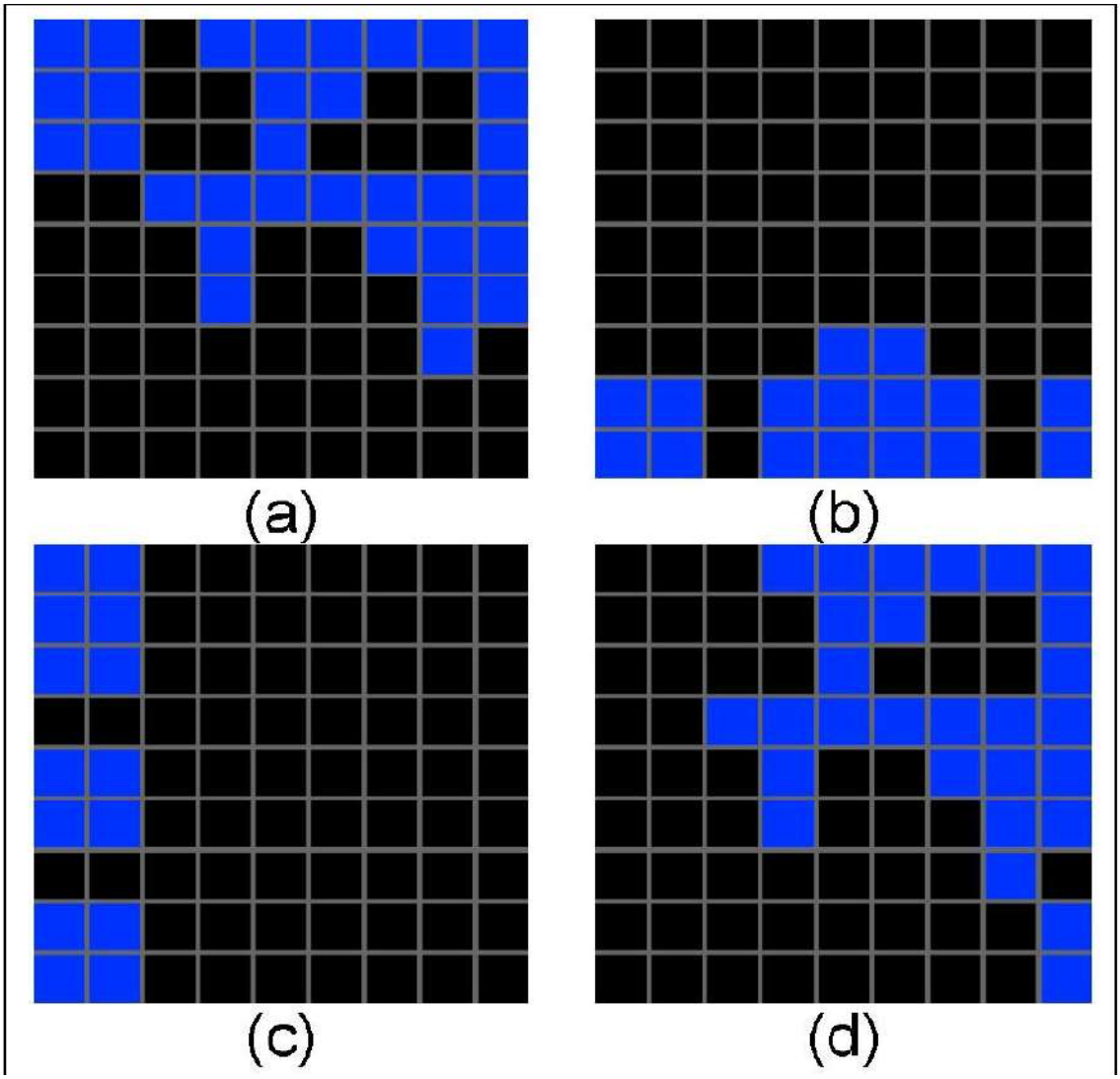

Figure 4. Pictures taken after performing the SA. Blue boxes represent the flooded scenario; (a) (T2B); (b) (B2T); (c) (L2R); (d) (R2L).

Results and discussions

Geometric change in local as well as regional faults affects the tectonically active drainage systems. The entire drainage network of northern regions of Pakistan is under the influence of neotectonics activity. The drainage network analysis method can monitor active tectonic signals which cause erosion and surface deformation. The drainage network is spatially distributed in four classes which include branched, parallel, cut off and rectangular drainage systems. The geometric transitions in different phases of spatial drainage system occur due to tectonic activity, geological factors, climatic changes and spatio temporal method. The tectonic activity dominates in highly steep regions resulting in parallel drainage patterns. The relative uplift of topography of a region results in linear drainage patterns due to tectonics uplift. Different fractal methods such as LA, SA and FD determine the undisturbed fractal patterns. Figure 5, 6 and 7 shows different values of FD, LA and SA respectively. The low value of FD indicates erosion processes and relative tectonic uplift. The value of FD up to 1

Matlab algorithm and Arc GIS applications generated the map for the distribution of FD by Box Counting Method. FD map is characterized by low to very low fractal value indicating high surface deformation and active tectonics. The high fractal values indicate low surface deformation due to active tectonics. North East (NE) zones of Skardu and Ghanche show high fractal values and non linear drainage patterns.

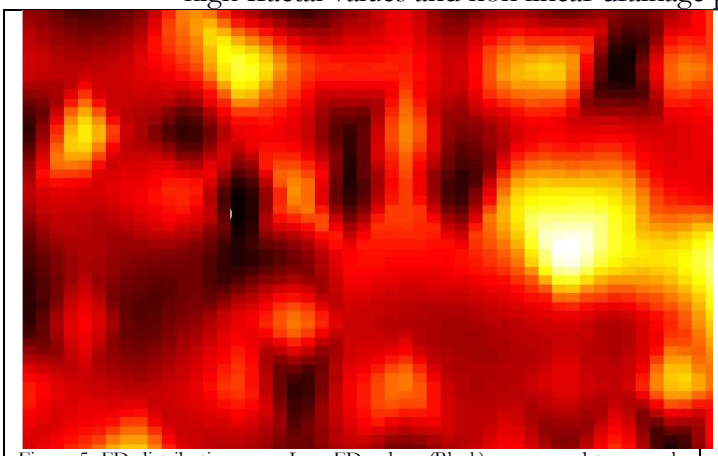

Figure 5: FD distribution map. Low FD values (Black) correspond to severely deformed zones shaded in black.

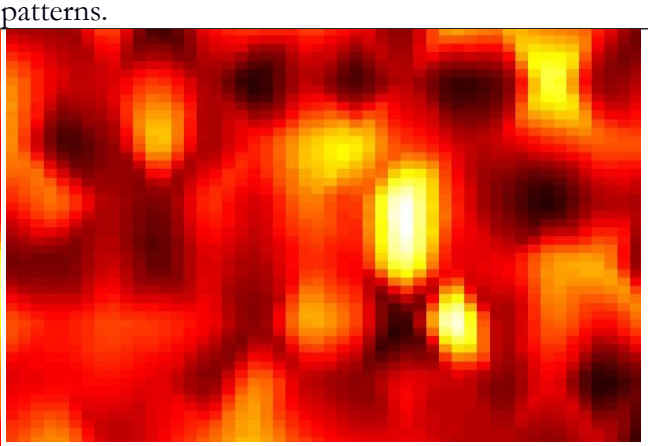

Figure 6: Distribution of map for LA values Low LA values are in black, red are medium and yell

Figure 8 indicates the topographic surface roughness of different structures using map of area under study. Presence of snow and glaciers in the western side of Hunza indicates high fractal value. Varying patterns of drainage networks result in varying FD values. Though the gaps between drainage pattern are distributed varyingly but spatial drainage network exhibit homogenous fractal values.The LA method monitors highly steep regions which are severly deformed by relative uplift. The regions deviating from the transitional behavior of patterns exhibited by drainage networks indicate high values of LA.

The regions exhibiting high fractal values correspond to high to medium values of LA. The GB regions have faced severe deformation due to collision of India Eurasia and current earthquake events. The surface deformation of streams and rivers due to neotectonics indicates the presence of thrusts and faults. Succolarity develops in the regions having similar fractal values of drainage network.The values of SA categorize different GB zones on the bases of structural orientation.

Surface topographic map portrays strong river incision in upper SkarduDeosai, upper Hunza, Plateau, Ghanche and Diamir-Gilgit-Astore indicating active tectonics and relative uplift along RaikotSassi fault. The collision of Eurasian and Indian plates causes thickening of earth's crust causing relative uplift and development of mountain chain. This process indicates incision and consequential neotectonics activity.

Conclusion

The fractal tools accurately report the spatial drainage network and topographic evolution in northern regions of Pakistan. The high LA and SA value and lower value of FD indicates high surface deformation and neotectonics activity in spatially distributed drainage networks. The fractal tools analyze the relative surface deformation accurately. The drainage network of Gilgit Baltistan displays parallel, disconnected and linear patterns of spatially distributed drainage networks in correspondence to active tectonics. The fractal tools indicated that Gilgit Baltistan is under impact of neotectonics activity and deforming severely. Increased

incision in Hunza valleys, Ghizer, Ghanche and upperSkardu causes sudden variations in Gilgit Baltistan region. Exceptionally, Deosai Plateau contains less incised regions. The increased incision represents high value of surface roughness and relative uplift. Surface roughness significantly appears in Hunza fault, MKT, RSF and along Karakorum fault. Computation of surface roughness through DEM provides efficient map to indicate neotectonics activity.

Acknowledgment

The authors are thankful to remote sensing and GIS laboratories of the Space Sciences Department, university of the Punjab, Lahore, Pakistan, for providing necessary facilities and field work support.

References

1. Melo, R. H. C., Conci, A., Identificação de tumoursdosseiospelaanálise de suasimagens on IEncontro Nacional de EngenhariaBiomecânica -ENEBI Organized by: ABCM, UFMG and IME. 2007.
2. Shahzad, F. and R. Gloaguen. TecDEM: A new tool for Tectonic Geomorphology, Part2: Surface dynamics and basin analysis.Computer and Geosciences. 2010.
3. Plotnick, R.E., Gardner, R.H., O'Neill, R.V., Lacunarity indices as measures of landscape texture, Landscape Ecology, Springer Netherlands, vol. 8, pp: 201-211, 1993.
4. Dombradi, E., G. Timar, B. Gabor, C. Sierd and H. Frank. Fractal dimension estimations of drainage network in the CarpathianPannonian system, Global and Planetary Change, Vol 58, issue 1-4, pp :197-213, 2007.
5. Dong, P..Lacunarity analysis of raster datasets and 1D, 2D. Computers and Geosciences, Vol 35, issue 10, pp: 2100-2110, 2009.
6. Grohmann, C. H.,.Morphometric analysis in Geographic Information Systems: applications of free software GRASS and R., Computers & Geosciences, Vol 30, pp :1055–1067, 2004.
7. Valous, N.A., D.W. Sun, P. Allen and F. Mendoza..The use of lacunarity for visual texture characterization of pre-sliced cooked pork ham surface intensities. Food Research International Vol 43, pp: 387–395, 2010.
8. Mahmood, S.A., F. Shahzad and R. Gloaguen..Remote sensing analysis of quaternary deformation using river networks in Hindukush region. In: IEEE International Geosciences and Remote Sensing Symposium, Cape Town, South Africa. Pp: II-369 - II-372, 2009.
9. Holschneider, M. On the wavelet transformation of fractal objects. Journal of Statistical Physics, Vol 50, issue 5, pp.963-993, 1988.
10. Theiler, J., 1990. Estimating fractal dimension. JOSA A, 7(6), pp.1055-1073.
11. Plotnick, R.E., Gardner, R.H. and O'Neill, R.V., Lacunarity indices as measures of landscape texture. Landscape ecology, Vol 8, issue 3, pp.201-211, 1993.
12. Plotnick, R.E., Gardner, R.H., Hargrove, W.W., Prestegaard, K. and Perlmutter, M., Lacunarity analysis: a general technique for the analysis of spatial patterns. Physical review E, Vol 53, issue 5, pp:5461, 1996.
13. De Melo, R.H.C. and Conci, A., Succolarity: Defining a method to calculate this fractal measure. In 2008 15th International Conference on Systems, Signals and Image Processing, pp. 291-294, 2008.
14. deMelo, R.H. and Conci, A., How succolarity could be used as another fractal measure in image analysis. Telecommunication Systems, Vol 52, issue3, pp.1643-1655, 2013.

15. Xia, Y., Cai, J., Perfect, E., Wei, W., Zhang, Q. and Meng, Q., 2019. Fractal dimension, lacunarity and succolarity analyses on CT images of reservoir rocks for permeability prediction. Journal of Hydrology, Vol 579, pp:124198, 2019.